METEORITICS & PLANETARY SCIENCE

High crustal diversity preserved in the lunar meteorite Mount DeWitt 12007 (Victoria Land, Antarctica)

Journal:	*Meteoritics & Planetary Science*
Manuscript ID	MAPS-2341.R2
Manuscript Type:	Article
Date Submitted by the Author:	n/a
Complete List of Authors:	Collareta, Alberto; Università di Pisa, Dipartimento di Scienze della Terra D'Orazio, Massimo; Università di Pisa, Dipartimento di Scienze della Terra Gemelli, Maurizio; Università di Pisa, Dipartimento di Scienze della Terra; Maurizio Gemelli, Pack, Andreas; Georg-August-Universität Göttingen, Geowissenschaftliches Zentrum, Abteilung Isotopengeologie Folco, Luigi; Università di Pisa, Dipartimento di Scienze della Terra
Keywords:	DEW 12007, mingled breccia, lunar regolith, Moon

UNIVERSITÀ DI PISA
DIPARTIMENTO DI SCIENZE DELLA TERRA

Pisa, October the 30th, 2015

Dear Editor, we submit a revised version of the manuscript:

"High crustal diversity preserved in the lunar meteorite Mount DeWitt 12007 (Victoria Land, Antarctica)"

by Alberto Collareta, Massimo D'Orazio, Maurizio Gemelli, Andreas Pack, and Luigi Folco for publication in *Meteoritics & Planetary Science*.

We accepted all Your useful advices and remarks, thus improving the main text, the captions and the tables. Please find enclosed a file detailing our most significant modifications.

We hope that this revised version of our paper will be suitable for publication in Your journal.

Sincerely Yours,

the Corresponding Author

Maurizio Gemelli

Researcher

Earth Science Department

Pisa University

e-mail address: maurizio.gemelli@unipi.it

High crustal diversity preserved in the lunar meteorite Mount DeWitt 12007 (Victoria Land, Antarctica)

Alberto COLLARETA[1,2], Massimo D'ORAZIO[1], Maurizio GEMELLI[1,*], Andreas PACK[3], and Luigi FOLCO[1]

[1]Dipartimento di Scienze della Terra, Università di Pisa, via S. Maria 53, 56126 Pisa, Italy
[2]Dottorato Regionale in Scienze della Terra Pegaso, Università di Pisa, via S. Maria 53, 56126 Pisa, Italy
[3]Georg-August-Universität Göttingen, Geowissenschaftliches Zentrum, Abteilung Isotopengeologie, Goldschmidtstraße 1, 37073 Göttingen, Germany

*Corresponding author. E-mail: maurizio.gemelli@unipi.it

Abstract – The meteorite Mount DeWitt (DEW) 12007 is a polymict regolith breccia mainly consisting of glassy impact-melt breccia particles, gabbroic clasts, feldspathic clasts, impact and volcanic glass beads, basaltic clasts and mingled breccia clasts embedded in a matrix dominated by fine-grained crystals; vesicular glassy veins and rare agglutinates are also present. Main minerals are plagioclase (typically $An_{>85}$) and clinopyroxene (pigeonites and augites, sometimes interspersed). The presence of tranquillityite, coupled with the petrophysical data, the O-isotope data ($\Delta^{17}O$ = -0.075) and the FeO_{tot}/MnO ratios in olivine (91), pyroxene (65) and bulk rock (77) indicate a lunar origin for DEW 12007. Impactites consist of Al-rich impact melt splashes and plagioclase-rich meta-melt clasts. The volcanic products belong to the Very Low Titanium (VLT) or Low Titanium (LT) suites; an unusual subophitic fragment could be cryptomare-related. Gabbroic clasts could represent part of a shallow intrusion within a volcanic complex with prevailing VLT affinity. DEW 12007 has a mingled bulk composition ~~and shows~~with relatively high incompatible element abundances ~~. DEW 12007~~and shows a high crustal diversity~~:~~, comprising clasts from the ~~major~~ Moon's major terranes and rare lithologies. First-order petrographic and chemical features suggest that DEW 12007 could be launch-paired with other meteorites including Y 793274/981031, QUE 94281, EET 87521/96008, and NWA 4884.

Keywords: DEW 12007, mingled breccia, lunar regolith, Moon, Antarctica

INTRODUCTION

The lunar crust is a unique window into early planetary differentiation processes in the solar system, bridging the gap between incipient igneous activity in asteroids and the more evolved geodynamics and differentiation of terrestrial planets like the Earth. Furthermore, it provides

significant insights into the cratering history ~~in the~~ of near Earth space. More than 45 years after the return of the first rock samples from the Moon, the architecture and diversity of the lunar crust still remains an outstanding question. The more than 380 kg of lunar specimens provided by the epic Apollo and Luna missions permitted a deep investigation of a tiny percentage of the Moon's nearside surface which resulted in the establishment of a somewhat reductionist lunar paradigm (i.e., the Moon surface has been viewed as substantially bimodal, consisting of heavily cratered plagioclase-rich highlands and circular, relatively featureless maria built up of basaltic lava floods). In the last decades, lunar science received new impulse by remote sensing missions (e.g., the *Clementine* and *Lunar Prospector* spacecrafts) and discovery of lunar meteorites (or lunaites). In fact, lunar meteorites represent a valuable extension to the Apollo and Luna sampling of the Moon surface, from a geographical and a geological point of view (Warren 1998). In October 2015, 233 officially named lunar meteorites were ~~censed~~ in the Meteoritical Bulletin Database (MBD). Of these meteorites, ~50% are feldspathic breccias, which probably originated (at least most of them) in the anorthositic highlands, ~25% are brecciated or unbrecciated basalts, and the remaining ~25% show intermediate petrographic and chemical compositions (Korotev et al. 2009). The latter group comprises both 'mingled' breccias (i.e., mechanical mixtures of highland feldspathic impactites, mare basalts and KREEP-rich materials) and breccias whose mafic components originated far from the lunar nearside mare basins and KREEPy terranes, and even in regions of the farside of the Moon (e.g., the South Pole Aitken basin; Mercer et al. 2013).

A new ~~lunar~~ meteorite (Fig. 1a) was recovered in Antarctica during the XXVIII Antarctic Austral Summer Campaign of the Italian Programma Nazionale di Ricerche in Antartide (PNRA). The discovery took place on January 3, 2013 on a blue ice patch 40 km due WSW of Mount DeWitt (77°14.153'S, 158°2.218'E), Victoria Land, during a joint PNRA/KOREAMET (Korean Expedition for Antarctic Meteorites, Republic of Korea) expedition. The 94.2 g ellipsoidal stone, partially covered by a thin and fresh dark fusion crust and devoid of evidence of apparent weathering, exhibited a brecciated structure. The meteorite, named Mount DeWitt 12007 (DEW 12007), turned out to be lunar, as recently announced by us in the Meteoritical Bulletin Database (http://www.lpi.usra.edu/meteor/metbull.php?code=59546).

In this paper, we expand on the first characterization of DEW 12007 (Collareta et al. 2014) reporting on its petrography, mineralogy, petrophysical properties, bulk chemistry and oxygen isotope data. We then discuss its classification and petrogenesis, its relationships to similar lunar meteorites and its possible source region on the lunar crust.

MATERIALS AND METHODS

DEW 12007 (Fig. 1a) is a fresh, oblate (7 × 3 × 3 cm) stone of 94.2 g. A 47.5 g endcut of the meteorite (nearly half specimen) is maintained by the Museo Nazionale dell'Antartide of the University of Siena (MNA-SI, Italy) for conservation and research purposes, while the remaining 46.7 g endcut is maintained by the Korea Polar Research Institute (KOPRI, Republic of Korea). About 7% of the external surface is covered by a greenish to dark brown vesicular fusion crust (Fig. 1b). The remaining surface shows a brecciated structure with abundant mm-sized white and pale gray clasts embedded in a dark gray fine-grained matrix. On freshly cut surfaces, a high diversity of variously colored and textured lithic and monomineralic fragments can be seen (Fig. 1c). Clasts are typically mm-sized or smaller and show a strongly ~~etherometric~~ heterometric size distribution. There is no evidence of depositional fabrics, but a moderate tendency to clast iso-orientation; roughly parallel to these lineations, a set of discontinuous, non-~~-~~pervasive fractures can be observed.

The 47.5 g endcut of DEW 12007 was cut in slices and then in part slices at MNA-SI using a low-velocity saw (South Bay Technology Model 650). A polished thin section of 170 mm^2 and four polished thick sections totaling about 370 mm^2 were prepared at MNA-SI laboratories for mineralogical and petrographic analyses. A 2.5 g part slice, taken from the interior of the meteorite, was finely grounded in an ~~virgin~~ agate mortar and pestle for whole rock chemical analyses. A 33 mg chip devoid of apparent large clasts from the interior of the meteorite was devoted to oxygen isotope analyses.

The petrographic investigations were conducted at the Dipartimento di Scienze della Terra of the University of Pisa (DST-UNIPI, Italy) using an optical microscope (OM) Zeiss Axioplan with transmitted and reflected light, and a microanalytical Scanning Electron Microscope (SEM) Philips XL30 coupled with an X-ray energy-dispersive spectrometer. The abundances of the various components of DEW 12007 were estimated by examining mosaics of Back-Scattered Electron (BSE) images of four sectioned and polished surfaces totaling more than 350 mm^2.

The bulk density ρ_b of DEW 12007 was determined by immersion of the main mass of the meteorite (36.7 g) in type 1 ultrapure water (*Milli-Q*) at T ~20 °C for less than 10 s; the main mass was then immediately dried in a vacuum chamber for 12 hours. The porosity, η_t, of DEW 12007 was determined using a point-counting technique similar to that used by Warren (2001). The technique is an application of BSE images acquired in two different series:

- I series: 10 random images, magnification 100×, dimensions: 1024 × 800 pixels;
- II series: 10 random images, magnification 4000×, dimensions: 512 × 400 pixels.

Series I was used to estimate the ~~gouge~~gross porosity η_g (attributable to the main fractures and vesicles), series II was used to estimate the fine porosity η_f (attributable to the microfractures and to the smaller vesicles). The 20 images were then ~~binarized~~ converted to binary images by coloring

voids in black, and mineral and glassy phases in white. This allowed us to quantify the porosity of every image as the percentage of black pixels. The total porosity η_t was then calculated as proposed by Warren (2001):

$$\eta_t = \eta_g + 0.75 \cdot \eta_f$$

Once obtained η_t, we calculated the grain density ρ_g of DEW 12007 as follows:

$$\rho_g = \rho_b / (1 - \eta_t)$$

The measurement of the magnetic susceptibility, χ, (mass-normalized and, as such, expressed in m^3/kg) of DEW 12007 was carried out with the pocket contact probe SM30 (ZH instruments). The main mass of DEW 12007 was positioned in different orientations with respect to the sensor of the susceptivimeter, and 12 measurements were taken. For each measurement a Log χ value was calculated applying the algorithm proposed by Gattacceca et al. (2004). Finally, a mean Log χ value was calculated.

Mineral and glass compositions were obtained by means of Electron Probe Micro-Analyzer (EPMA). The analyses were conducted at Istituto di Geoscienze e Georisorse (IGG-CNR) in Padua (Italy) using a CAMECA SX50 instrument fitted with four wavelength dispersive spectrometers. Running conditions were: accelerating voltage, 20 kV; beam current, 20 nA; counting time, 10 s (peak) + 5 s (background); ~~only~~ for ~~the~~ determin~~ation~~ing ~~of~~n Na, K, Si and Al in glasses, a beam current of 2 nA and a counting time of 10 s (background) ~~was~~~~ere~~were applied. The nominal beam spot was 5 μm for the analyses of all minerals; defocussed beam spots of 10 μm were used for glasses. A number of synthetic and mineral standards were used for instrumental calibration.

The major-element bulk composition of DEW 12007 was determined by Fusion-XRF at ACTLABS (Ancaster, Ontario, Canada). The loss on ignition (LOI) was determined at ACTLABS igniting the sample at 1050 °C for 2 hours.

The concentrations of 35 trace elements were determined by Inductively Coupled Plasma-Mass Spectrometry (ICP-MS) (Perkin Elmer NexION 300x) at DST-UNIPI. About 20 to 50 mg of samples were dissolved in PFA vessels on a hot plate using ultrapure HF and HNO_3. The sample solutions were measured by external calibration using the international geochemical reference sample BE-N (alkali basalt) for calibration. Two aliquots of DEW 12007 whole rock powder and two clasts (named clast S and clast L) were analyzed by ICP-MS.

The oxygen isotope composition of DEW 12007 was determined at Geowissenschaftliches Zentrum (Georg-August-Universität Göttingen, Germany) by laser fluorination in combination with dual inlet gas source mass spectrometry. The liberated O_2 was cleaned from contaminants by means of cold traps and gas chromatography. Experimental values are given as $\delta^{17}O$, $\delta^{18}O$, and $\Delta^{17}O$ notation. The δ values describe the per mil (‰) deviation from the international standard, V-SMOW:

$$\delta^{x}O = [(({}^{x}O/{}^{16}O)_{sample}/({}^{x}O/{}^{16}O)_{VSMOW}) - 1] \cdot 10^{3}$$

where X = 18 or 17.

The $\Delta^{17}O$ is calculated relative to a reference line with slope 0.5305 and zero intercept (see Pack and Herwartz, 2014) with

$$\Delta^{17}O = 10^{3} \cdot \ln(\delta^{17}O \cdot 10^{-3} + 1) - 0.5305 \cdot 10^{3} \cdot \ln(\delta^{18}O \cdot 10^{-3} + 1)$$

The errors in $\delta^{17}O$ and $\delta^{18}O$ are about ± 0.15 and ± 0.2 ‰ (note that these errors are correlated) and the error in $\Delta^{17}O$ is ~ ± 0.01 ‰ (errors given as 1σ). For details of the technique, see Pack and Herwartz (2014).

RESULTS

Magnetic susceptibility, density and porosity

The results of the petrophysical investigations conducted on DEW 12007 are reported in Table 1. It is possible to compare the magnetic susceptibility of DEW 12007 (Log χ = 3.11 ± 0.9 10^{-9} m^3/kg) with the characteristic ranges of the various meteorite classes provided by Folco et al. (2006). The magnetic susceptibility of DEW 12007 is fully compatible with a lunar origin, but it does not exclude its attribution to other classes of differentiated achondrites (i.e., HED or SNC meteorites).

Assuming that DEW 12007 wa~~i~~s lunar, we made a comparison with the database of 37 lunar meteorites (including mare basalts, highland feldspathic breccias and mafic breccias) studied by Rochette et al. (2010) by means of magnetic measurements. The Log χ of DEW 12007 rules out a parentage with highland feldspathic breccias and mare basalts, whereas it is perfectly compatible with a classification within the mafic breccias. A similar result is obtained when plotting Log χ, ρ_g (= 3.02 ± 0.03 g cm^{-3}), and η_t (= 4.1 ± 1.1 vol.%) of DEW 12007 in the magnetic susceptibility versus grain density and porosity versus grain density spaces. In these two diagrams (Figs. 2a, 2b) DEW 12007 is located within the field of the non-feldspathic, non-basaltic lunar breccias measured by Macke et al. (2011).

Oxygen isotope composition

The $\Delta^{17}O$ of DEW 12007 is -0.075±0.010‰, which is within 2σ error identical to the -0.089 ± 0.002‰ suggested by Herwartz et al. (2014) for the Moon (Table 1). Note that following the scheme suggested by Pack and Herwartz (2014), terrestrial mantle rocks plot at $\delta^{18}O$ ~ 5.5 ‰ and $\Delta^{17}O$ = -0.101 ‰, whereas the typical values of $\Delta^{17}O$ shown by martian and vestoid meteorites are significantly higher and significantly lower than -0.075 respectively by about 0.2 ‰. The O

isotopes are hence consistent with a lunar origin of DEW 12007.

Petrography and mineralogy

From a micro-structural point of view, DEW 12007 is a polymict breccia consisting of mm-sized or smaller lithic clasts immersed in an aphanitic matrix. The main typologies of clasts include (in order of decreasing abundance): glassy melt breccia clasts, plagioclase-rich clasts, crystalline basaltic clasts, medium-grained gabbroic clasts, impact and volcanic glass beads (discriminated according to the criteria provided by Delano (1986)), clinopyroxene-olivine-silica symplectitic associations and mingled breccia clasts. The fragmental fraction of the matrix is dominated by very fine-grained fragments; vesicular glassy veins (which cement the meteorite) and rare agglutinates are also present. No granulometric hiatus can be observed between the largest clasts and the fragments of the matrix. The main minerals are plagioclase and clinopyroxene (augites and pigeonites, sometimes interspersed) followed by olivine, ilmenite, Al-bearing ulvöspinel, troilite, silica polymorphs and Al-bearing chromite. Minor phases include tiny grains of baddeleyite, tranquillityite, phosphates, Fe,Ni-metal alloys (both taenite and kamacite) and schreibersite. All the constituents of the breccia show various degrees of impact-related modifications. Shock features span widely from fracturing to undulatory extinction to planar deformation features (PDFs) in plagioclases and, less frequently, in pyroxenes (Fig. 3), and to diaplectic glass.

A summary of the texture and mineralogy of the main constituents of DEW 12007 is given in Table 2~~3~~. In the following paragraphs we present a more detailed description of the main type of clasts found in DEW 12007 in order of decreasing abundance.

Lithic clasts

Glassy impact-melt breccias

Glassy impact-melt breccias (e.g., Fig. 4a) are among the most abundant lithologies in DEW 12007. They are observed in the meteorite as polyhedral or ellipsoidal mm-sized clasts consisting of an extremely heterogeneous vitrophyric groundmass in which some lithic and mineral fragments (sub-clasts) are immersed. These sub-clasts, which are badly-defined schlieren under the optical microscope, are easily recognizable under the SEM; they make approximately 10 vol.% of the glassy breccia clasts. Lithic subclasts are basaltic and plagioclase-rich particles. Mineral fragments are predominantly calcic plagioclase (An_{91-97}), clinopyroxene (highly magnesian augite and pigeonite), and olivine (Fo_{76-84} or below Fo_{15}). Some glassy breccia clasts include fragments of a mafic Al-bearing phase whose chemistry is compatible with a pyroxene rich in Ca-Tschermak

component. The latter is known to be an important component of the lunar clinopyroxenes formed at high temperature and relatively low pressure (Okamura et al. 1974). Some clasts show spherules of Fe,Ni-metal in the groundmass. A few clasts show very rare sub-clasts, and could be more properly classified as crystal-poor impact-melts. Following Papike et al. (1998), the impact-melt breccias in DEW 12007 could be attributed to episodes of local impact-related melting of 'mingled' basaltic-feldspathic protoliths.

Plagioclase-rich clasts

Plagioclase-rich clasts (e.g., Fig. 4b) comprise various lithic fragments typically 1-5 mm in size. They contain approximatively 50 to 75 vol.% of fine- (~100 μm) to very fine-grained (~10 μm) calcic plagioclase ($An_{>85}$) and maskelynite immersed in a mafic groundmass. The groundmass is made of moderately magnesian clinopyroxenes (augites and pigeonites, zoned and not interspersed) and a mafic Al-bearing glass (Table 34); minor phases include oxides (ilmenite and baddeleyite) and tiny grains of Fe,Ni-metal, troilite, and schreibersite. Most of these lithic fragments are very similar to the so-called "meta-melt" clasts observed by some authors (Koeberl et al. 1990; 1996; Day et al. 2006) in various mafic lunar regolith breccias; those clasts have been interpreted as thermometamorphic impactites (partially melted fine-grained granulites) deriving from brecciated, feldspar-rich, nonmare source rocks.

Two of these granulitic clasts (clast S and clast L) have also been analysed by means of ICP-MS in order to determine their trace-element compositions. Clast S (fig. 4b) contains *ca*. 75 vol.% of fine to very fine grained stick-like, locally maskelynized anorthitic plagioclase individuals. The groundmass of clast S is constituted by two mafic phases, i.e., a clinopyroxene and a homogeneous, non-vesiculated Al-rich glass, plus rare interstitial ilmenite. Clast L differs from clast S by: *i*) being more texturally heterogeneous, *ii*) showing a higher plagioclase/matrix ratio (~1), and *iii*) presenting slightly higher abundances of ilmenite, Fe,Ni-metal, and baddeleyite.

The modal composition of the plagioclase-rich clasts of DEW 12007 can be described as gabbroic-anorthositic. Their mineral chemistry, in terms of Mg# ((Mg# = molar MgO/(MgO + FeO_{tot}) × 100)) in mafic phases vs An% in plagioclase (Fig. 5), links most of them (including clast L) to the rocks of the so-called Mg-suite; the highly feldspathic clast S could instead be associated to a ferroan anorthositic protolith.

Crystalline basalts

Crystalline sub-mm sized basalt fragments are ubiquitous components of DEW 12007. They show a large textural variability, yet with a rather monotonous and homogeneous mineral

composition. Basaltic micro-textures span from hypocrystalline to holocrystalline, from hyalopilitic to microglomerophyritic, from microporphyritic to intergranular, ophitic and variolitic (e.g., Figs. 4c-4e). All of the basaltic clasts are composed of anorthitic plagioclase (An_{92-97}; Table 4~~5~~), pigeonite (Table ~~6~~5) and/or mafic glass with accessory Cr- and Ti-bearing oxides. The crystalline basalts in DEW 12007 can be classified as Very Low Titanium (VLT) and Low Titanium (LT) basalts. An unusual medium-grained subophitic-glomerophyritic particle (clast 8, Fig. 4e) shows a pyroxene-like Al-rich phase and rare, very small grains of baddeleyite, Fe,Ni-metal and troilite. The texture of clast 8 suggests a volcanic origin. However, the occurrence of some phases with considerable contents of highly siderophile elements (HSEs), such as Fe,Ni-metal, suggests a certain degree of meteoritic contamination or, in other words, an impact origin.

Due to the mineral chemistry of its pyroxenes and plagioclases, clast 8 is related to the Mg-rich (*sensu* Papike et al. 1998) nonmare lunar rocks; therefore, if volcanic, clast 8 could represent a cryptomare-related crystalline basalt.

Gabbroic clasts

Various mm-sized, medium-grained lithic fragments show a quasi-pristine igneous microgranular phaneritic texture. These clasts (e.g., Fig. 4f) are dominated by zoned clinopyroxene (En_{36-55}, Wo_{13-39}, Table 5~~6~~) and anorthitic plagioclase (An_{90-94}, Table 4~~5~~). The latter exhibits undulose extinction; it is often recrystallized and locally transformed into maskelynite. Minor components include euhedral silica (probably tridymite, according to morphological and optical observations), chromite and tiny grains of baddeleyite, tranquillityite (a characteristic phase of the lunar maria), a phosphate (probably whitlockite) and Si-, K-rich melt inclusions; gabbroic clasts lack ilmenite and orthopyroxene. Pyroxene mineral chemistry indicates that gabbroic clasts are unrelated to nonmare Mg-gabbronoritic rocks. Indeed the pyroxene of the latter are generally strongly magnesian ($En_{>65}$) and bordered by orthopyroxene; moreover nonmare Mg-gabbronoritic rocks typically are rich in ilmenite and/or olivine (James and Flohr 1983). In fact, gabbroic clasts in DEW 12007 could be better related to the VLT volcanic clasts recognized within the meteorite.

Volcanic glass beads

Ovoidal, small-sized (≤ 0.5 mm) brownish glass beads (e.g., Fig. 4g) are frequent constituents of DEW 12007. These clasts are optically homogeneous or display very fine-grained quenching microtextures characterized by hopper and dendritic microcrystals embedded in glass. They show small compositional variability and high Mg/Al atomic ratios (~1.9). According to Delano (1986), they can be interpreted as pyroclastic glass beads originated by hawaiian-style eruptions (i.e., 'lava fountains') within a mare volcanic complex. Their glass chemistry (Table 6~~7~~) reveals a picritic

composition and a low degree of intra- and inter-sample chemical variability; all the analyzed beads are VLT volcanic glasses (Figs. 6a-6b). One volcanic glass bead contains three tiny (< 100 μm) euhedral crystals of forsteritic olivine ($Fo_{\sim 80}$). These individuals are most probably crystallized from the encasing melt; in fact, the VLT crystalline products often shows forsteritic olivine ($Fo_{\sim 75}$), and this phase is believed to occur on the liquidus curve of most VLT magmas (Vaniman and Papike, 1977).

Impact glass spherules

Some mm-sized glass spherules (e.g., Fig. 4h) occur in DEW 12007. They are translucent with perlaceous luster, and present teal to light blue colors in reflected light. These glass spherules are homogeneous (or nearly so) and do not bear important schlieren or inclusions. The composition of two of these objects (vt 1 and vt 2) were determined by EPMA transects. On the basis of their sizes and low Mg/Al atomic ratio they can be classified as impact glass particles deriving from the melting of Al-rich nonmare protolites. The bulk chemistry of sample vt 1 matches that of the Apollo impact glasses and pure ferroan anorthosites (Table 7~~8~~ and Fig. 7). The identification of the source rock of glass particle vt 2 is more difficult; its somewhat anomalous bulk composition with high Al (Al_2O_3 = 20.4 wt%) and high Ti (TiO_2 = 1.90 wt%) could derive from the melting of a Mg-, Ti-rich nonmare rock, or from a mixture of ANT and basaltic (LT?) end members.

Clinopyroxene-olivine-silica symplectitic associations

Sub-mm sized, very fine-grained symplectitic clasts are characteristic constituents of DEW 12007 (Fig. 4i). They are composed of very tiny (generally < 20 μm) crystals of fayalitic olivine and a silica phase immersed in a groundmass of moderately ferriferous, medium-Ca augite. Among these clasts, those which show abundant clinopyroxene, exhibit sandwich-like, elongated silica-olivine-silica intergrowth textures. Furthermore, a few of them contain Si-, K-rich melt inclusions analogous to those observed in some gabbroic clasts. Overall, these clasts strongly resemble pyroxferroite-breakdown symplectitic products (e.g., Aramovich et al. 2001). However, the Fs component of the pyroxene is too low ($En_{20\text{-}25}$, $Fs_{55\text{-}65}$) to result from the breakdown of pyroxferroite. It is in turn likely that these associations resulted from the exsolution of a metastable, medium-Ca pyroxene. On the basis of the presence of distinctive acidic, potassic melt inclusions and of their crystal chemistry, these partially exsolved clinopyroxenes can be associated to those of the gabbroic clasts.

Fragmental breccia clasts

Fragmental breccia clasts are rare constituents of the meteorite. They are sub-mm sized

polygonal aggregates (e.g., Fig. 4j) of fine- to very fine-grained (generally < 10 μm) angular mineral particles (sub-clasts). No granulometric hiatus can be observed between the coarser sub-clasts and the finer ones. These fragments are bounded together by a very thin film of glass. Where the glass is relatively thick it is invariably highly vesiculated. Main phases are plagioclase (Ca-rich anorthite), olivine (forsterite) and clinopyroxene (namely, augite and pigeonite). A peculiar chondrule-like sub-clast occurs within a single fragmental breccia clast. It is a ~200 μm ellipsoidal particle composed of parallel bands of fine-grained, dove-shaped, quenched olivine crystals connected by plagioclase sticks immersed in a microcrystalline (clinopyroxene-, fayalite-rich?) groundmass. This sub-clast is quite different from the so-called "lunar chondrules" (e.g., Symes et al. 1998) and could represent the product of the quenching of a volcanic magma droplet with picritic composition.

Matrix

Mineral fragments

The fragmental fraction of the matrix of DEW 12007 is composed by angular monomineralic particles which show a rather high mineralogical diversity. Silicate fragments are typically from ~200 to a few μm in size and show a seriate grain size distribution. Clinopyroxene and plagioclase are the main phases (Table ~~5~~4 and Table 5~~6~~). All the analyzed plagioclases are $An_{>85}$, but a single individual is An_{70}. A coarse grained (~1 mm long), euhedral, chemically homogeneous, plagioclase fragment (An_{94}) was also observed.. Most plagioclase particles in the matrix are optically disturbed and a few of them present PDFs or are amorphous. Pyroxene fragments are medium- to slightly high-Fe (Fs_{25}-Fs_{65}) augite and pigeonite; Ca abundances span widely (Wo_{12}-Wo_{40}), with apparent continuity within the most ferriferous pyroxenes. Pyroxene individuals which show coarse (μm-sized) exsolution lamellae are abundant. Olivine particles show forsterite contents either below Fo_{16} or between Fo_{50}-Fo_{90}. With respect to the whole meteorite, the matrix is relatively enriched in non-silicate phases (oxides, Fe,Ni-metal, sulfides, phosphides and phosphates). Most oxides are ilmenite and chromite, which typically form subhedral, ~100 μm sized, crystal fragments; ulvöspinel and baddeleyite are also well represented but less abundant. Ulvöspinel and chromite often show high Al contents (a characteristic chemical anomaly of lunar Fe-Cr-oxides according to Papike et al. 1998). Fe,Ni-metal, sulfides, and phosphides form tiny grains; their abundance could be both due to a certain degree of meteoritic contamination and to their refractory behavior. Some EPMA analyses of the non-silicate mineral fragments of the matrix are reported in Table 8~~9~~.

Glass veins

DEW 12007 is cemented by a network of glass veins (e.g., Fig. 4k), veinlets and films that constitute the amorphous fraction of the matrix. The majority of the veins, typically 1 mm long and 0.1 mm thick, are randomly oriented, highly heterogeneous and vesiculated; vesicles are generally tens of μm in diameter. They contain partially digested lithic and mineral fragments; flow structures and vesicle trails are also present. These veins can be interpreted as formed by injection and propagation within the lunar soil of a liquid phase formed by shock melting of the regolith. The bulk composition of the veins (Table 9~~10~~) is similar to that of the bulk meteorite. Minor chemical differences between different veins could reflect local heterogeneity of the finest fraction of the regolith source materials, associated with high cooling rates and thus low degree of mixing. Older generations of veins characteristically cut and border some clasts.

Agglutinates

Some equidimensional, sub-mm sized aggregates of fine particles bonded together by vesiculated glass occur in DEW 12007. A few of them are well distinguishable from the matrix and can be easily recognized as pristine agglutinates. Most of them, however, form instead vesicular regions with indistinct boundaries with the bordering glass veins (e.g., Fig. 4k). These aggregates can be interpreted as 'quasi-collapsed agglutinates'.

Fusion crust

DEW 12007 preserves cm-sized patches of the fusion crust (Fig. 1b, Fig. 4l). This consists of a ~0.3 mm thick, extremely vesiculated, glass envelope. Vesicles are generally 1-50 μm in diameter, and their size increases outwards. Locally, the outer edge of the fusion crust is smooth and not vesiculated. The glass is remarkably homogeneous. Relic crystals (especially oxides) and ~1 μm sized microcrystals with quenched textures (dove-shaped, aligned olivine crystals; cross-shaped oxides and metallic droplets) are locally observed. Texturally, the fusion crust of DEW 12007 is thus quite similar to that of the polymict eucrite ALHA76005 described by Genge and Grady (1999). The glass composing the fusion crust of DEW 12007 is remarkably similar to that of the whole rock in terms of major-element bulk composition (Table 1~~1~~0), yet the former is slightly depleted in Fe. This minor chemical difference could be related to a substrate heterogeneity (Thaisen and Taylor 2009), or to a preferential Fe fractionation into Fe-oxide dendrites.

Geochemistry

The major-element bulk composition of DEW 12007 is presented in Table 1~~2~~1. It confirms that

DEW 12007 is a lunar meteorite. The key ratio FeO_{tot}/MnO (77.3) falls within the typical range of lunar meteorites (60 < FeO_{tot}/MnO < 80); moreover, the FeO_{tot} and MnO contents of DEW 12007 are not compatible with an origin from Mars (FeO_{tot}/MnO ~ 40) or from asteroid 4 Vesta (FeO_{tot}/MnO ~ 30).

The bulk trace-element composition of DEW 12007 and that of the plagioclase-rich granulitic particles clast L and clast S are presented in Table 1~~3~~2. The chondrite-normalized rare earth elements (REEs) pattern of DEW 12007 is almost rectilinear (Fig. 8a), showing a slight negative anomaly of Eu (Eu/Eu* = 0.78) and moderate degree of fractionation ($[La/Yb]_n$ = 2.0). The overall pattern of clast S (Fig. 8a) is very similar to that of the bulk meteorite, except for the absence of the negative Eu anomaly. Clast L is ~3 times more enriched in all the rare earth elements than the bulk meteorite and its REE pattern (Fig. 8a) shows a more marked negative anomaly of Eu (Eu/Eu* = 0.52). Clast S and clast L, so similar from a textural and mineralogical point of view, are therefore characterized by very different enrichments in REEs: in terms of lunar rock geochemistry, they are very differently enriched in the KREEP component. Similar observation can be extended to the other incompatible element contents. The spider diagrams of Fig. 8b show that clast S, clast L and the bulk meteorite have incompatible element patterns which share a similar overall trend of increasing abundances towards the most incompatible elements. The composition of clast S mimics that of the bulk meteorite, while showing slightly higher contents of most incompatible elements. Clast L shows higher enrichments in all the determined incompatible elements, with a significant depletion of Sr with respect to the bulk meteorite.

DISCUSSION

Classification of DEW 12007

DEW 12007 can be classified as a lunar meteorite on the basis of: *i*) its magnetic susceptibility (Log χ = 3.11 ± 0.9, with χ expressed in 10^{-9} m^3/kg) coupled with its first-order petrographic features; *ii*) its oxygen isotope composition ($\Delta^{17}O$ = -0.075 ‰); *iii*) FeO_{tot}/MnO ratios in olivine (~91), pyroxene (~65) and bulk rock (~77). This classification is also corroborated by the occurrence of typical lunar lithologies (e.g., feldspathic granulites and high-alumina impact glasses) and minerals (e.g., tranquillityite).

DEW 12007 fails the test proposed by Korotev (2005a) for basaltic lunaites, but fully satisfies that regarding non-basaltic lunaites: in fact, FeO_{tot} = 12.6 wt% < 15 wt%, and Eu (µg/g) ~ 0.75 + 0.056 · Sm (µg/g) (see Tables 1~~0~~1 and 1~~1~~2). However, DEW 12007 is not anorthositic ~~*sensu*~~

following the definition by Korotev (2005a) ~~definition~~, because CaO/Al_2O_3 ~ 0.7 > 0.5. Furthermore, DEW 12007 does~~is~~ not fit the definition of ~~a~~ highland rock ~~either~~ according to either Norman (2009) or ~~according to~~ Rochette et al. (2010); in fact Al_2O_3 = 18.3 wt% < 20 wt% and FeO_{tot} = 12.6 wt% > 8 wt%.

As reported above, the petrophysical properties of DEW 12007 suggest that this meteorite can be classified as a non-basaltic, non-feldspathic, intermediate mafic breccia. This classification is largely confirmed by plotting the chemical composition of DEW 12007 in the diagrams proposed by Korotev (http://meteorites.wustl.edu/). Furthermore, it perfectly matches the petrography of the meteorite, which shows a mechanical mixture of nonmare mafic and plagioclase-rich materials as well as mare basaltic ones (Fig. 9). On the basis of the observation of the typical constituents of the lunar soil, we conclude that DEW 12007 can be classified as a mingled regolith breccia. In this view, the quite high FeO_{tot}/MnO ratio of the bulk rock could reflect a certain degree of extralunar meteoritic contamination (see discussion below): in fact, the average solid fraction of the solar system has a Fe/Mn value of ~94 (Anders and Grevesse 1989). Note that, while the FeO_{tot}/MnO ratio of the bulk meteorite (~77) is quite high with respect to all the lunar meteorites (~68), the FeO_{tot}/MnO ratios of pyroxene (~65) and olivine (~91) are almost indistinguishable from those characteristic of lunar pyroxene and olivine (~66 and ~90 respectively) reported by Papike (1998). This suggests that the relatively high FeO_{tot}/MnO ratio of the bulk meteorite is not a genuine lunar magmatic signature, but the contribution of exotic Fe-bearing phases in the fragmental fraction of the DEW 12007 matrix and in some impactitic clasts. If refined and formalized, this observation could lead to the definition of a new, simple, chemical index of maturity of the lunar regolith (and regolith breccia), based on the comparison of the FeO_{tot}/MnO ratios in the bulk rock with those in the pyroxenes and olivines. However, the intermediate values of Log χ and Ni content (Fig. 10) suggest that the degree of meteoritic contamination in DEW 12007 is moderate. This indicates that DEW 12007 is a not a completely mature regolith, i.e., ~~which~~ it experienced some kind of early lithification.

On the basis of the observation of some relict agglutinates, we can assume that the regolith sampled by DEW 12007 was shock-lithified at P < 20 kbar. In fact, according to various authors (e.g., Simon et al. 1986), shock melting of the lunar soil typically results in the complete collapse of the agglutinates at P ≥ 20 kbar.

~~Note that, while the FeO_{tot}/MnO ratio of the bulk meteorite (~77) is quite high with respect to all the lunar meteorites (~68), the FeO_{tot}/MnO ratios of pyroxene (~65) and olivine (~91) are almost indistinguishable from those characteristic of lunar pyroxene and olivine (~66 and ~90 respectively) reported by Papike (1998). This suggests that the relatively high FeO_{tot}/MnO ratio of the bulk meteorite is not a genuine lunar magmatic signature, but the contribution of exotic Fe-bearing~~

~~phases in the fragmental fraction of the DEW 12007 matrix and in some impactitic clasts. If refined and formalized, this observation could lead to the definition of a new, simple, chemical index of maturity of the lunar regolith (and regolith breccia), based on the comparison of the FeO_{tot}/MnO ratios in the bulk rock with those in the pyroxenes and olivines.~~

Among the other lunar meteorites with intermediate iron contents, DEW 12007 shows rather high REEs contents and a moderate negative Eu anomaly which could be a reflection of a very low abundance of FAN anorthositic material.

DEW 12007 is distinct from roughly three quarters of other known lunaites due to its intermediate composition. Furthermore, present data indicate that DEW 12007 is not paired with any other known meteorite. Even the nearest recovered (~44 km away) Antarctic lunar meteorite, ALH 81005, although being an anorthositic breccia, strongly differs from DEW 12007 in terms of petrography and geochemistry.

The mare crust

The most characteristic basaltic constituents of DEW 12007 are crystalline and glassy basalts pertaining to the VLT mare volcanic suite and, subordinately, to the LT suite. However, there is good evidence to associate the gabbroic clasts observed in DEW 12007 with the VLT basalts:

1) The lack of ilmenite, a quasi-ubiquitous phase in lunar materials, suggests that the gabbroic clasts are very poor in Ti, much more than the gabbronoritic rocks of the so-called Mg-suite (James and Flohr 1983).

2) The occurrence of tranquillityite, a typical accessory phase of mare basalts (e.g., Papike et al. 1998), relates the gabbroic clasts to the mare magmatism.

3) The Mg-suite related rocks observed in DEW 12007 are impactites that show a granulitic thermometamorphic textural overprint. In turn, the texture of the gabbroic clasts is microgranular, i.e., a pristine magmatic microstructure.

4) In the diagram proposed by Nielsen and Drake (1978) (Fig. 11a), the pyroxenes from the gabbroic clasts plot far from the field of the "highland" pyroxenes, overlapping the compositional trends for VLT and, subordinately, LT mare basalts.

On the basis of these observations, we propose that the gabbroic clasts in DEW 12007 represent part of a shallow intrusion within a mare volcanic complex with prevailing VLT affinity. A similar interpretation was proposed by Jolliff et al. (1998) with regard to the gabbroic clasts found in the lunar regolith breccia Queen Alexandra Range 94281.

Note that many of the pyroxenes in the matrix of the DEW 12007 have a VLT-like mineral composition, and seem to comprise and expand the compositional variability of the pyroxenes of

the gabbroic clasts (Fig. 11a). A similar observation can be made in the En-Fs-Di-Hd diagram (Fig. 11b). Thus, the matrix of DEW 12007 is likely partly composed of mineral particles deriving from the comminution of the gabbroic clasts observed in the meteorite. This interpretation is supported by the occurrence of silica-phosphate clasts, i.e., assemblages exclusively found within gabbroic clasts.

The mare crust components of DEW 12007 are weakly shocked extrusive and hypabyssal rock particles which sample a VLT-like volcanic complex from its sub-surface intrusive bodies to its crystalline and glassy eruptive products. We thus suggest that the volcanic and subvolcanic VLT clasts are autochthonous materials within the DEW 12007 regolith.

The nonmare crust

The plagioclase-rich meta-melt rocks (post-impact granulites as defined by Koerbel et al., 1990) and the aluminous glass particles found in DEW 12007 represent a nonmare crust composed mainly of mafic feldspar-bearing rocks attributable to the so-called Mg-suite. The ICP-MS analyses of two feldspathic clasts (clast S and clast L) showed two very different REE and incompatible element patterns (Fig. 8a, Fig. 8b). While clast L shows a strong KREEPy fingerprint such as those observed in some non ordinary lunar magnesian rock devoid of olivine (e.g., Papike et al. 1998), the REE pattern of clast S (for which a FAN source rock has been hypothesized) is puzzling: the absence of Eu anomaly (Eu/Eu* = 0.99), coupled with relatively high elemental enrichments (La~30 times CI abundance, $[La/Yb]_n$ ~2) are very strange in the lunar scenario. We compared clast S with an anorthositic-gabbroic particle studied by Laul et al. (1983). The latter presents La~20 times CI abundance, $[La/Yb]_n$~2 and no Eu anomaly. Following Laul et al. (1983), we propose that clast S derived from a FAN protolith moderately contaminated by a KREEP component.

The Al-rich granulitic and glassy clasts in DEW 12007 depict a rather diverse and original nonmare crustal assemblage, which consists mainly of mafic rocks of the so-called Mg-suite (including some KREEP-rich terms), plus KREEPy, FAN-derived, gabbroic-anorthositic meta-melt rocks and pure highland lithologies, such as FAN anorthositic glasses.

Launch pairing and the source area of DEW 12007

A number of lunar meteorites could be genetically related to DEW 12007 including Yamato (Y) 793274/981031 (paired meteorites), Yamato (Y) 793169, Queen Alexandra Range (QUE) 94281, Meteorite Hills (MET) 01210, Elephant Moraine (EET) 87521/96008 (paired meteorites), Miller Range (MIL) 05035, Northwest Africa (NWA) 4884, and Asuka (A) 881757.

Arai and Warren (1999) established the Y 793274/981031 and QUE 94281 launch pair (namely: a group of two or more meteorites ejected from the parent body by the same impact event) by identifying two populations of VLT pyroclastic glasses (labeled YQ1 and YQ2) that occur in both meteorites. Furthermore, Korotev et al. (2003a; 2003b) proposed that Y 793274/981031 and QUE 94281 could likely be launch-paired with EET 87521/96008. The close launch ages (~0.05 Ma, according to CRE ages reported by Arai and Warren, 1999) for Y 793274/981031, QUE 94281 and EET 87521 supports this putative launch-pairing group (YQ/EET). Recently, Korotev et al. (2009) and Korotev and Zeigler (2014) provided strong compositional arguments supporting an even larger launch-pairing group (YQEN) which includes the Antarctic YQ/EET meteorites and NWA 4884 from the Sahara Desert. Despite the limited petrographic and minerochemical information available to date, the lithophile element distribution of NWA 4884 is identical to that of QUE 94281 (Korotev et al. 2009).

Some authors have suggested the so-called YAMM launch-pairing group (Y 793169, Asuka 881757, MIL 05035, and MET 01210), which possibly samples a complete stratigraphic section ranging from the uppermost regolith layer to the underlying lava products (Arai et al. 2010). The meteorites belonging to the YAMM group present close launch ages of ~1 Ma (significantly older than those of the YQ/EET meteorites) (Arai et al. 2010).

Finally, Korotev and Zeigler (2014) recently proposed that various lunar basalts - namely: NWA 032/479 (paired meteorites), NWA 4734, LaPaz Icefield (LAP) 02205/02224/02226/02436/03632/04841 (paired meteorites) - could come from the same ejection site (NNL putative launch-pairing group).

Being a mingled regolith breccia, DEW 12007 shows more or less pronounced petrological and geochemical affinities with all the aforementioned~~said~~ intermediate to basaltic lunar meteorites belonging to the YQEN and YAMM putative launch-pairing groups. In particular, from a petrographic point of view, DEW 12007 is strikingly similar to QUE 94281. QUE 94281 is a glassy-matrix, clast-rich regolith breccia consisting of a mechanical mixture of basaltic, mare-related components and feldspathic, nonmare-related material. The clastic fraction of QUE 94281 is dominated by mineral fragments which presumably originated within a shallow intrusion (or thick lava flow) in a mare context (Jolliff et al. 1998). Among these mineral fragments, coarse-grained pyroxene clasts are prominent; they are typically exsolved, presenting μm-thick exsolution lamellae (Jolliff et al. 1998). The chemical composition of the pyroxenes clasts follows a Fe-enrichment trend which suggests slow cooling rates, relating them to the VLT suite lunar rocks (Jolliff et al. 1998). Most of the mineral fragments of QUE 94281 were thus referred to a "VLT gabbro" source rock by Jolliff et al. (1998). Lithic clasts in QUE 94281 include VLT basalts and gabbros, glass particles (both picritic pyroclastic glass droplets and Al-rich impact melt splashes), glassy to

cryptocrystalline Al-rich impact melt breccias, and other feldspathic impactites; agglutinates and vesicular glass veins are also present (Jolliff et al. 1998; Arai and Warren 1999; Korotev et al. 2009; Korotev and Zeigler 2014).

The presence of VLT gabbros is the most obvious feature which relates DEW 12007 to QUE 94281; other remarkable common features include the prominence of subrounded, feldspathic to mafic impact melt breccia clasts, the texture and chemical composition of the pyroxene fragments, the presence of agglutinates, the mineral chemistry of the main phases, the major- and trace-element bulk meteorite composition (Fig. 8a, Fig. 8b).

VLT-like gabbroic clasts are also present in Y 793274/981031 and in EET 87521/96008. Their bulk REE and incompatible element patterns is virtually indistinguishable from those of DEW 12007 (Fig. 8a, Fig. 8b). Note that EET 87521/96008 are characterized by the presence of peculiar clasts consisting of clinopyroxene, fayalite and silica intergrowths (Anand et al. 2003). These components are texturally identical to those present in DEW 12007 and described by us as clinopyroxene-olivine-silica symplectitic associations (see above). Last but not least, the major-element composition of the VLT glass beads found in DEW 12007 fully matches that of the YQ1 population of volcanic glasses found in both Y 793274/981031 and QUE 94281 (0.37-0.63 wt% TiO_2, 10-17 wt% MgO, and 9-11 wt% Al_2O_3).

In the 2-element diagrams provided by Korotev and Zeigler (2014) for the YAMM and YQEN lunaites, DEW 12007 plots along the mixing line defined by the YQEN meteorites between two end-members: a VLT-like, mare-related component and a Mg-rich, nonmare-related component (Fig. 12). In these geochemical spaces, DEW 12007 lies within the compositional field proper of the YQEN meteorites, near the feldspathic end-member.

Therefore, due to the overall petrographic and compositional similarity and the ubiquitous occurrence of peculiar clasts, we propose that the possibility of a wide launch-pairing group consisting of Y 793274/981031, QUE 94281, EET 87521/96008, NWA 4884 and DEW 12007 should be carefully explored by detailed comparative petrographic studies and producing CRE data for DEW 12007. Within this putative launch-pairing group, DEW 12007 is most similar to QUE 94281, Yamato 793274/981031, and possibly NWA 4884 (whose petrography is still not known in detail to date), since they sample a more aluminous regolith than EET 87521/96008. The latter feature likely implies a more important contribution of materials from the nonmare feldspathic terranes (that is, a shallow position within the regolith column).

DEW 12007 is a regolith breccia and thus it can be compared with remote sensing geochemical data collected over the Moon surface to constrain its provenance. We modified the method of Joy et al. (2011) and Mercer et al. (2013) choosing to use the low spatial resolution (5° per pixel) *Clementine* Ti and Fe ultraviolet-visible-infrared (UVVIS) datasets. We did not use the high spatial

resolution (0.5° per pixel) *Lunar Prospector* Th and Fe gamma-ray spectrometer datasets, because DEW 12007 is Th-poor (Th = 1.11 μg g^{-1}) and the *Lunar Prospector* data notoriously overestimate Th contents in regions with low Th concentrations (Warren 2005). We searched the *Clementine* UVVIS datasets (accessed at http://www.lpi.usra.edu/lunar/missions/clementine/) using bulk composition parameters of 0.62 ± 1 wt% TiO_2 and 12.6 ± 1 wt% FeO. The resulting maps (Fig. 13, elaborated through the interpolation of the *Clementine* data via Delaunay triangulation) indicate that DEW 12007 is similar, in terms of Ti and Fe contents, to areas *i*) near the western and northern boundaries of Oceanus Procellarum, *ii*) within Mare Imbrium (near Sinus Iridum, Plato crater and Archimedes crater), *iii*) in correspondence of the northern region of Mare Serenitatis, *iv*) at the centre of Mare Fecunditatis and *v*) in the northwestern part of Mare Crisium. Note that the general context of these areas - inside mare basins, but near the mare-nonmare transition - is consistent with our interpretation of the regolith sampled by DEW 12007.

The high-KREEP regolith of Oceanus Procellarum and Mare Crisium, dominated by the High Titanium (HT) and LT volcanic rocks, is particularly enriched in incompatible elements and typically shows high Th contents. This is not compatible with the geochemistry of DEW 12007. In turn, the Apollo and Luna missions have shown that Mare Serenitatis, Mare Fecunditatis and Mare Crisium are regions of more or less developed VLT volcanism. Note that these three maria were also ~~individuated~~ identified by Calzada-Diaz et al. (2015) as possible source areas for the lunar mingled meteorites comprised in the so-called YAMM group.

If, following Korotev (2000, 2005b), we identify the Procellarum KREEP Terrane (and not the feldspathic highlands) as the source area for the so-called Mg-suite of "highlands" rocks (at least for the KREEP-rich, HSE-bearing ones), an association between DEW 12007 and the regolith developed on a VLT volcanic complex sited within Mare Serenitatis (possibly near the mare-nonmare boundary) can be proposed. In this location, the regolith could have collected both autochthonous, mare-related, materials and Al-rich impact ejecta from the proximal KREEPy nonmare regions (Mare Procellarum and Mare Imbrium) and feldspathic highlands (Fig. 14). However, any further investigation of the source area of DEW 12007 should consider its genetic relationships with the other non-feldspathic lunar meteorites.

CONCLUSIONS

1) Petrophysical properties, petrographic data, bulk chemical composition, and oxygen isotope composition indicate that DEW 12007 is a lunar meteorite, confirming our previous report in abstract form (Collareta et al. 2014).

2) DEW 12007 can be classified as a mingled regolith breccia, containing materials from both

mare and nonmare terranes, which developed on a VLT volcanic complex near a magnesian feldspathic terrane. DEW 12007 is unpaired and distinct from roughly three quarters of other known lunaites for its intermediate composition.

3) Our petrographic and minerochemical investigations show that DEW 12007 samples a high diversity of crustal rocks, including clasts from the major Moon terranes (the Feldspathic Highland Terrane, the Procellarum KREEP Terrane and the basaltic maria) and some rare lunar materials (i.e., a putative pre-mare volcanic clast and some VLT-like gabbroic clasts).

4) A first-order petrographic and geochemical comparison suggests that a possible launch-pairing relationship between DEW 12007 and other mingled lunar meteorites (Y 793274/981031, QUE 94281, EET 87521/96008 and NWA 4884) should be properly investigated.

5) On the basis of *Clementine* remote sensing compositional data and major petrographic and geochemical features, a region near the margin of Mare Serenitatis could likely represent the geological context for the formation and the ejection of DEW 12007; however, similar locations within Mare Fecunditatis or Mare Crisium could be other plausible options.

6) A comparison between the FeO_{tot}/MnO ratios in mafic minerals (olivine and pyroxene) and bulk rock suggests the former is a more robust tool for rapid identification of the planetary parentage of achondritic meteorites.

Acknowledgments—This work is supported by the Italian *Programma Nazionale delle Ricerche in Antartide* (PNRA) through the PEA2013 AZ2.04 "Meteoriti Antartiche". Luigi Folco and Massimo D'Orazio research is also supported by Pisa University's *Fondi di Ateneo*. The Museo Nazionale dell'Antartide in Siena (MNA-SI) provided the samples for this study. Raul Carampin provided valuable EPMA assistance. We thank Sergio Rocchi, and Mahesh Anand for fruitful discussions. Reviews by Randy L. Korotev, Guy J. Consolmagno, Kevin Righter, and Gretchen Benedix greatly improved this paper.

References

Anand M., Taylor L. A., Neal C. R., Snyder G. A., Patchen A., Sano Y., and Terada K. 2003. Petrogenesis of lunar meteorite EET 96008. *Geochimica et Cosmochimica Acta* 67:3499-3518.

Anders E., and Grevesse N. 1989. Abundances of the elements: meteoritic and solar. *Geochimica et Cosmochimica acta* 53:197-214.

Arai T., and Warren P. H. 1999. Lunar meteorite Queen Alexandra Range 94281: Glass compositions and other evidence for launch pairing with Yamato 793274. *Meteoritics & Planetary Science* 34:209-234.

Arai T., Ray Hawke B., Giguere T. A., Misawa K., Miyamoto M., and Kojima H. 2010. Antarctic

lunar meteorites Yamato-793169, Asuka-881757, MIL 05035, and MET 01210 (YAMM): Launch pairing and possible cryptomare origin. *Geochimica et Cosmochimica Acta* 74:2231-2248.

Aramovich C. J., Herd C. D. K., and Papike J. J. 2001. Possible causes for late-stage reaction textures associated with pyroxferroite and metastable pyroxenes in the basaltic Martian meteorites (abstract #1003). In: Proceedings, 33rd Lunar and Planetary Science Conference.

Collareta A., D'Orazio M., Gemelli M., Pack A., and Folco L. 2014. The new lunar meteorite Mount DeWitt 12007 (abstract). *Meteoritics and Planetary Sciences* 47(Suppl.):5104.pdf.

Day J., Floss C., Taylor L. A., Anand M., and Patchen A. D. 2006. Evolved mare basalt magmatism, high Mg/Fe feldspathic crust, chondritic impactors, and the petrogenesis of Antarctic lunar breccia meteorites Meteorite Hills 01210 and Pecora Escarpment 02007. *Geochimica et cosmochimica acta* 70:5957-5989.

Delano J. W. 1986. Pristine lunar glasses: criteria, data, and implications. *Journal of Geophysical Research: Solid Earth* 91:201-213.

Demidova S. I., Nazarov M. A., Lorenz C. A., Kurat G., Brandstätter F., and Ntaflos T., 2007. Chemical Composition of Lunar Meteorites and the Lunar Crust. *Petrology*, 15:386-407.

Folco L., Rochette P., Gattacceca J., and Perchiazzi N. 2006. In situ identification, pairing, and classification of meteorites from Antarctica through magnetic susceptibility measurements. *Meteoritics and Planetary Science* 41:343-353.

Gattacceca J., Eisenlohr P., and Rochette P. 2004. Calibration of in situ magnetic susceptibility measurements. *Geophysical Journal International* 158:42-49.

Genge M. J., and Grady M. M. 1999. The fusion crusts of stony meteorites: implications for the atmospheric reprocessing of extraterrestrial materials. *Meteoritics and Planetary Science* 34:341-356.

Herwartz D., Pack A., Friedrichs B., and Bischoff A. 2014. Identification of the giant impactor Theia in lunar rocks. *Science* 344:1146-1150.

James O. B., and Flohr M. K. 1983. Subdivision of the Mg-suite noritic rocks into Mg-gabbronorites and Mg-norites. *Journal of Geophysical Research: Solid Earth* 88:A603-A614.

Jolliff B. L., Korotev R. L., and Rockow, K. M. 1998. Geochemistry and petrology of lunar meteorite Queen Alexandra Range 94281, a mixed mare and highland regolith breccia, with special emphasis on very-low-Ti mafic components. *Meteoritics and Planetary Science* 33:581-601.

Joy K. H., Crawford I. A., Russel S. S., Swinyard B., Kellett B., and Grande M. 2006. Lunar regolith breccias MET 01210, PCA 02007 and DAG 400: their importance in understanding the lunar surface and implications for the scientific analysis of D-CIXS data (abstract #1274). 37th

Lunar and Planetary Science Conference. CD-ROM.

Joy K. H., Burgess R., Hinton R., Fernandes V. A., Crawford I. A., Kearsley A. T., and Irving A. J. 2011. Petrogenesis and chronology of lunar meteorite Northwest Africa 4472: a KREEPy regolith breccia from the Moon. *Geochimica et Cosmochimica Acta* 75:2420-2452.

Koeberl C., Kurat G., and Brandstätter F. 1990. Lunar meteorite Yamato-86032: Mineralogical, petrological, and geochemical studies. *Antarctic Meteorite Research* 3:3-18.

Koeberl C., Kurat G., and Brandstätter F. 1996. Mineralogy and geochemistry of lunar meteorite Queen Alexandra Range 93069. *Meteoritics and Planetary Science* 31:897-908.

Korotev R. L. 2000. The great lunar hot spot and the composition and origin of the Apollo mafic ("LKFM") impact-melt breccias. *Journal of Geophysical Research: Planets*, 105:4317-4345.

Korotev R. L., Jolliff B. L., Zeigler R. A., and Haskin L. A. 2003a. Compositional evidence for launch pairing of the YQ and Elephant Moraine lunar meteorites (abstract #1357). In: Proceedings, 44th Lunar and Planetary Science Conference.

Korotev R. L., Jolliff B. L., Zeigler R. A., and Haskin L. A. 2003b. Compositional constraints on the launch pairing of three brecciated lunar meteorites of basaltic composition. *Antarctic Meteorite Research* 16:152-175.

Korotev R. L. 2005a. Lunar geochemistry as told by lunar meteorites. *Chemie der Erde-Geochemistry* 65:297-346.

Korotev R. L. 2005b. The myth of the magnesian suite of lunar "highlands" rocks (abstract). *Meteoritics and Planetary Science* 40(Suppl.):A86.

Korotev R. L., Zeigler R. A., Jolliff B. L., Irving A. J., and Bunch T. E. 2009. Compositional and lithological diversity among brecciated lunar meteorite of intermediate iron concentration. *Meteoritics and Planetary Science* 44:1287-1322.

Korotev R. L., and Zeigler R. A. 2014. ANSMET Meteorites from the Moon. In Thirty-five Seasons of U.S. Antarctic Meteorites (1976–2010): A Pictorial Guide to the Collection, edited by Righter K., Harvey R. P., Corrigan C. M., and McCoy T. C. Washington, D. C.: Wiley. pp. 101-130.

Laul J. C., Papike J. J., Simon S. B., and Shearer C. K. 1983. Chemistry of the Apollo 11 highland component. *Journal of Geophysical Research* 88 (Suppl.):B139-B149.

Liu Y., Floss C., Day J. M. D., Hill E., and Taylor L. A. 2009. Petrogenesis of lunar mare basalt meteorite Miller Range 05035. *Meteoritics and Planetary Science* 44:261-284.

Macke R. J., Kiefer W. S., Britt D. T., Irving A. J., and Consolmagno G. J. 2011. Densities, porosities and magnetic susceptibilities of meteoritic lunar samples: early results (abstract #1986). In: Proceedings, 42nd Lunar and Planetary Science Conference.

McDonough W. F., and Sun S. S. 1995. The composition of the Earth. *Chemical geology*, 120:223-253.

Mercer C. N., Treiman A. H., and Joy K. H. 2013. New lunar meteorite Northwest Africa 2996: A window into farside lithologies and petrogenesis. *Meteoritics and Planetary Science* 48:289-315.

Morris R. V., See T. H., and Hörz F. 1986. Composition of the Cayley Formation at Apollo 16 as inferred from impact melt splashes. *Journal of Geophysical Research: Solid Earth* 91:E21- E42.

Nielsen R. L., and Drake M. J. 1978. The case for at least three mare basalt magmas at the Luna 24 landing site. In: Mare Crisium: The view from Luna 24; Proceedings of the Conference. pp. 419-428.

Norman M. D., and Taylor S. R. 1992. Geochemistry of lunar crustal rocks from breccia 67016 and the composition of the Moon. *Geochimica et Cosmochimica Acta* 56:1013-1024.

Norman M. D. 2009. The lunar cataclysm: Reality or "mythconception"? *Elements* 5:23-28.

Okamura F. P., Ghose S., and Ohashi H. 1974. Structure and crystal chemistry of Calcium Tschermak's pyroxene, CaAlAlSiO6. *American Mineralogist* 59:549-557.

Pack A., and Herwartz D. 2014. The triple oxygen isotope composition of the Earth mantle and understanding variations in terrestrial rocks and minerals. *Earth and Planetary Science Letters* 390:138-145.

Papike J. J. 1998. Comparative planetary mineralogy; chemistry of melt-derived pyroxene, feldspar, and olivine. *Reviews in Mineralogy and Geochemistry* 36:7.1-7.11.

Papike J. J., Ryder G., and Shearer C. K. 1998. Lunar samples. *Reviews in Mineralogy and Geochemistry* 36:5.1-5.234.

Rochette P., Gattacceca J., Ivanov A. V., Nazarov M. A., and Bezaeva N. S. 2010. Magnetic properties of lunar materials: meteorites, Luna and Apollo returned samples. *Earth and Planetary Science Letters* 292:383-391.

Shearer C. K., and Papike J. J. 1993. Basaltic magmatism on the Moon: a perspective from volcanic picritic glass beads. *Geochimica et Cosmochimica Acta* 57:4785-4812.

Simon S. B., Papike J. J., Hörz F., and See T. H. 1986. An experimental investigation of agglutinate melting mechanisms: shocked mixtures of Apollo 11 and 16 soils. *Journal of Geophysical Research: Solid Earth* 91:E64-E74.

Spicuzza M. J., Day J. M. D., Taylor L. A., and Valley J. W. 2007. Oxygen isotope constraints on the origin and differentiation of the Moon. *Earth and Planetary Science Letters* 253:254-265.

Symes S. J., Sears D. W., Akridge D., Huang S., and Benoit P. H. 1998. The crystalline lunar spherules: their formation and implications for the origin of meteoritic chondrules. *Meteoritics and Planetary Science* 33:13-29.

Taylor G. J. 2000. A new Moon for the twenty-first century. *Planetary Science Research Discoveries.* Accessed online at http://www.psrd.hawaii.edu/Aug00/newMoon.html.

Taylor S. R., Gorton M. P., Muir P., Nance W. B., Rudowski R., and Ware N. 1973. Composition of

the Descartes region, lunar highlands. *Geochimica et Cosmochimica Acta* 37:2665-2683.

Thaisen K. G., and Taylor L. A. 2009. Meteorite fusion crust variability. *Meteoritics and Planetary Science* 44:871-878.

Vaniman D. T., and Papike J. J. 1977. Very low Ti / VLT basalts: a new mare rock type from the Apollo 17 drill core. In: Proceedings, 8th Lunar and Planetary Science Conference. pp. 1443-1471.

Warren P. H., and Wasson J. T. 1978. Compositional-petrographic investigation of pristine nonmare rocks. In: Proceedings, 9th Lunar and Planetary Science Conference. pp. 185-217.

Warren P. H., Jerde E. A., and Kallemeyn G. W. 1987. Pristine Moon rocks: a “large” felsite and a metal-rich ferroan anorthosite. *Journal of Geophysical Research: Solid Earth* 92:E303-E313.

Warren P. H. 1998. A brief review of the scientific importance of lunar meteorites. In: Workshop on new views of the Moon: integrated remotely sensed, geophysical, and sample datasets (abstract #6047).

Warren P. H. 2001. Porosities of lunar meteorites: strength, porosity, and petrologic screening during the meteorite delivery process. *Journal of Geophysical Research: Planets* 106:10101-10111.

Warren P. H. 2005. “New” lunar meteorites: implications for composition of the global lunar surface, lunar crust, and the bulk Moon. *Meteoritics and Planetary Science* 403:477-506.

Wiechert U., Halliday A. N., Lee D. C., Snyder G. A., Taylor L. A., and Rumble D. 2001. Oxygen isotopes and the Moon-forming giant impact. *Science* 294:345-348.

Wieczorek M. A., Jolliff B. L., Khan A., Pritchard M. E., Weiss B. P., Williams J. G., Hood L. L., Righter K., Neal C. R., Shearer C. K., McCallum I. S., Tompkins S., Hawke B. R., Peterson C., Gillis J. J., and Bussey B. 2006. The constitution and structure of the lunar interior. *Reviews in Mineralogy and Geochemistry* 60:221-364.

Yanai K., and Kojima H. 1991. Varieties of lunar meteorites recovered from Antarctica. *Proceedings of the NIPR Symposium on Antarctic Meteorites* 4:70-90.

Captions

Figures

Fig. 1. The 94.2 g DEW 12007 lunar meteorite. a) Field photo of DEW 12007. b) Detail of the external surface of DEW 12007 showing a patch of fusion crust. c) Three freshly cut surfaces of DEW 12007 showing its internal structure (1 cm cube for scale).

Fig. 2. Diagrams, after Macke et al. (2011) showing magnetic susceptibility, grain density and porosity of DEW 12007 and other lunar specimens (Apollo samples and meteorites) for comparison. a) Log χ versus grain density. b) Porosity versus grain density.

Fig. 3. Plagioclase fragment from the matrix of DEW 12007. Dotted lines indicate three sets of planar deformation features (PDFs). Optical microscope (OM) image, crossed polars.

Fig. 4. SEM-BSE images of the most prominent constituents of DEW 12007. a) Glassy melt breccia. b) Plagioclase-rich clast (clast S). c) Microporphyritic pigeonite basalt. d) Sub-variolitic pigeonite basalt. e) Subophitic-glomerophyritic clast (clast 8). f) Gabbroic clast. g) VLT volcanic glass bead. h) Impact glass particle (clast vt 2). i) Symplectitic clinopyroxene-olivine-silica association. j) Fragmental breccia clast (note the chondrule-like object on the left margin of the clast). k) Glass vein with a highly vesiculated region ('quasi-collapsed agglutinate'). l) Vesiculated fusion crust. Abbreviations: ilm = ilmenite; msk = maskelynite; plg = plagioclase; px = pyroxene.

Fig. 5. Mg# (in mafic phases) versus An% (in plagioclase) diagram for the feldspar-rich meta-melt rock clasts in DEW 12007~~,~~ (~~clast S is~~see for example Fig. 4b~~–~~). Compositional fields after Wieckzorek et al. (2006).

Fig. 6. a) TiO_2 versus Mg# diagram and b) SiO_2 vs Mg# diagram for the volcanic glass beads of DEW 12007. Compositional fields after Papike et al. (1998). Squares, triangles and diamonds represent three different glass bead individuals (see for example Fig. 4g).

Fig. 7. Molar Na/(Na+Ca) × 100 vs Mg# diagram for the impact glass particle vt 1. Compositional fields for ferroan anorthosites and the Mg-suite rocks after Papike et al. (1998).

Fig. 8. a) CI chondrite-normalized REE patterns of DEW 12007 (bulk meteorite), clast S, clast L

and other lunar meteorites. b) Incompatible element patterns of DEW 12007 (bulk meteorite), clast S, clast L and other lunar meteorites. Normalizing values after McDonough and Sun (1995). Compositional data after: [1]Demidova et al. (2007), [2]Joy et al. (2006), [3]Anand et al. (2003), [4]Liu et al. (2009), [5]Yanai and Kojima (1991), [6]Korotev et al. (2009).

Fig. 9. DEW 12007 in the FeO_{tot} vs Al_2O_3 diagram. Modified after Korotev (http://meteorites.wustl.edu/).

Fig. 10. DEW 12007 in the Log Ni vs Log χ diagram in comparison with other lunar meteorites. Circles: feldspathic breccias; squares: mafic breccias; triangles: basalts. Modified after Rochette et al. (2010).

Fig. 11. Mineral chemistry of the pyroxene from gabbroic clasts and the meteorite matrix. a) Ti/(Ti + Cr) vs Fe/(Fe + Mn) diagram. b) Quadrilateral (En-Fs-Di-Hd) pyroxene diagram.

Fig. 12. Scandium, Th, Ti, versus Fe contents in DEW 12007 and other lunar meteorites belonging to the YAMM, NNL, and YQEN putative launch-pairing groups for comparison. The vertical dashed line discriminates between feldspathic and non-feldspathic meteorites. a) Ti vs FeO_{tot} diagram. b) Sc vs FeO_{tot} diagram. c) Th vs FeO_{tot} diagram. Plots modified after Korotev and Zeigler (2014).

Fig. 13. Search results for FeO between 11.6 and 13.6 wt% (green layer) and TiO_2 below 1.62 wt% (pink layer) using the Clementine datasets. Areas of overlap are red. On the left, the western hemisphere of the Moon; on the right, the eastern hemisphere of the Moon. Images obtained by Google Earth. Mare Serenitatis is located ca. 25°N-35°N, 5°E-25°E.

Fig. 14. In this image, modified after ~~the internet site http://www.psrd.hawaii.edu/~~Taylor (2000), the regolith sampled by DEW 12007 is contextualized in a schematic section of the lunar northern hemisphere crust and upper mantle passing through the northern basins (Oceanus Procellarum, Mare Imbrium, and Mare Serenitatis).

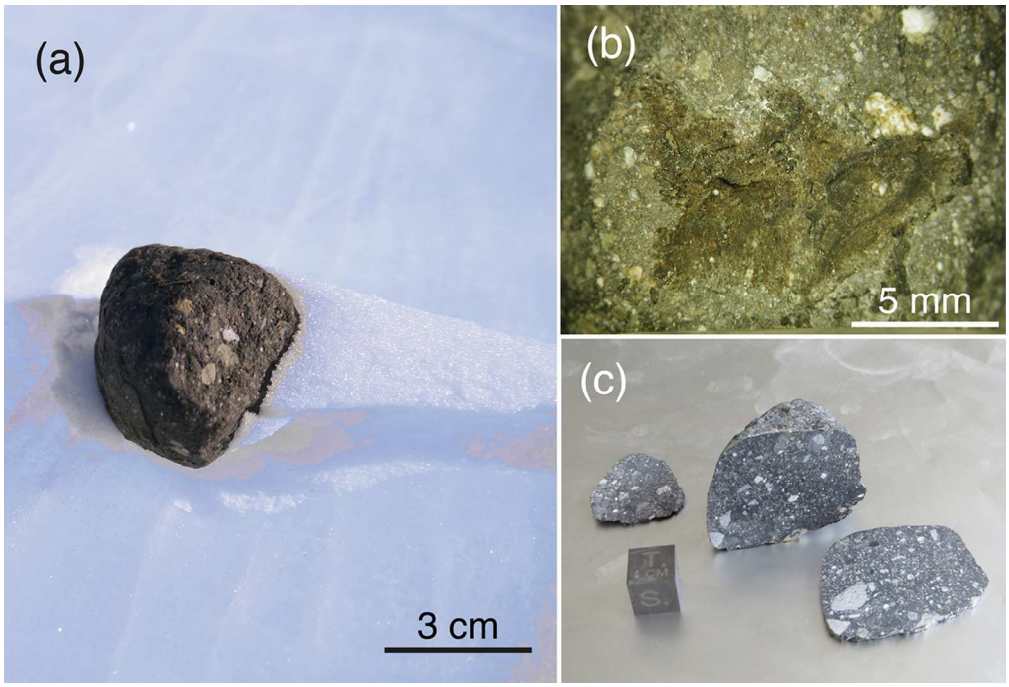

Fig. 1. The 94.2 g DEW 12007 lunar meteorite. a) DEW 12007 in the field. b) Detail of the external surface of DEW 12007 showing a patch of fusion crust. c) Three freshly cut surfaces of DEW 12007 showing its internal structure (1 cm cube for scale).
118x79mm (300 x 300 DPI)

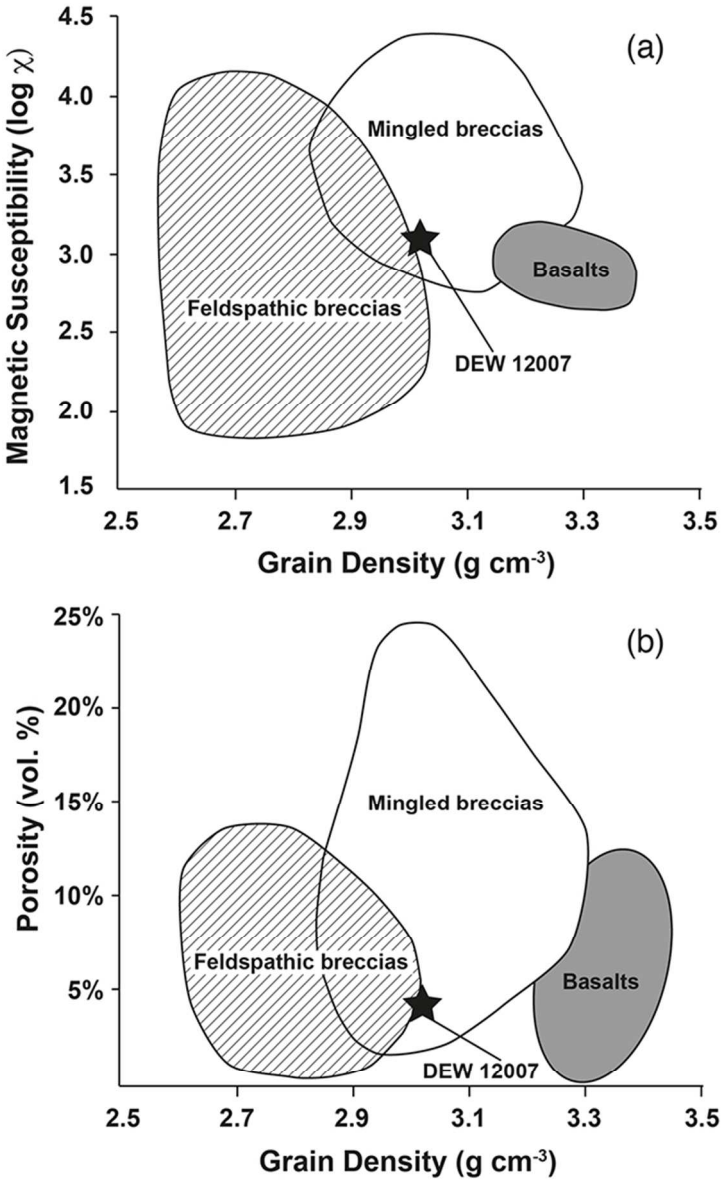

Fig. 2. DEW 12007 in two diagrams provided by Macke et al. (2011) in comparison with other lunar specimens (Apollo samples and meteorites). a) Log χ versus grain density. b) Porosity versus grain density. 58x93mm (300 x 300 DPI)

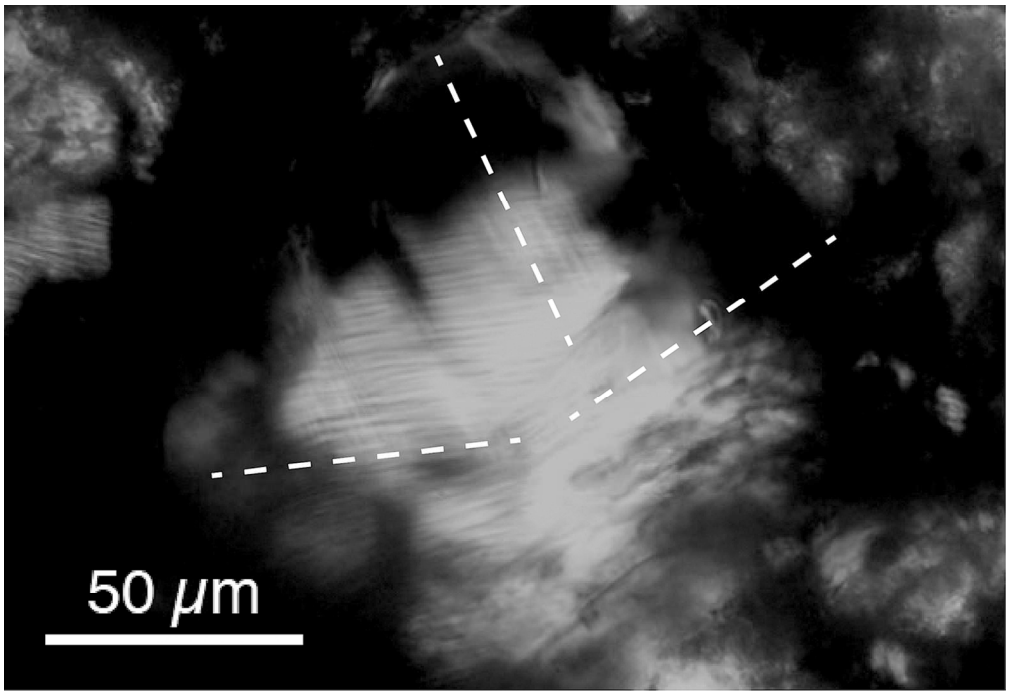

Fig. 3. Plagioclase fragment from the matrix of DEW 12007. Dotted lines indicate three sets of planar deformation features (PDFs). Optical microscope (OM) image, crossed polars.
122x83mm (300 x 300 DPI)

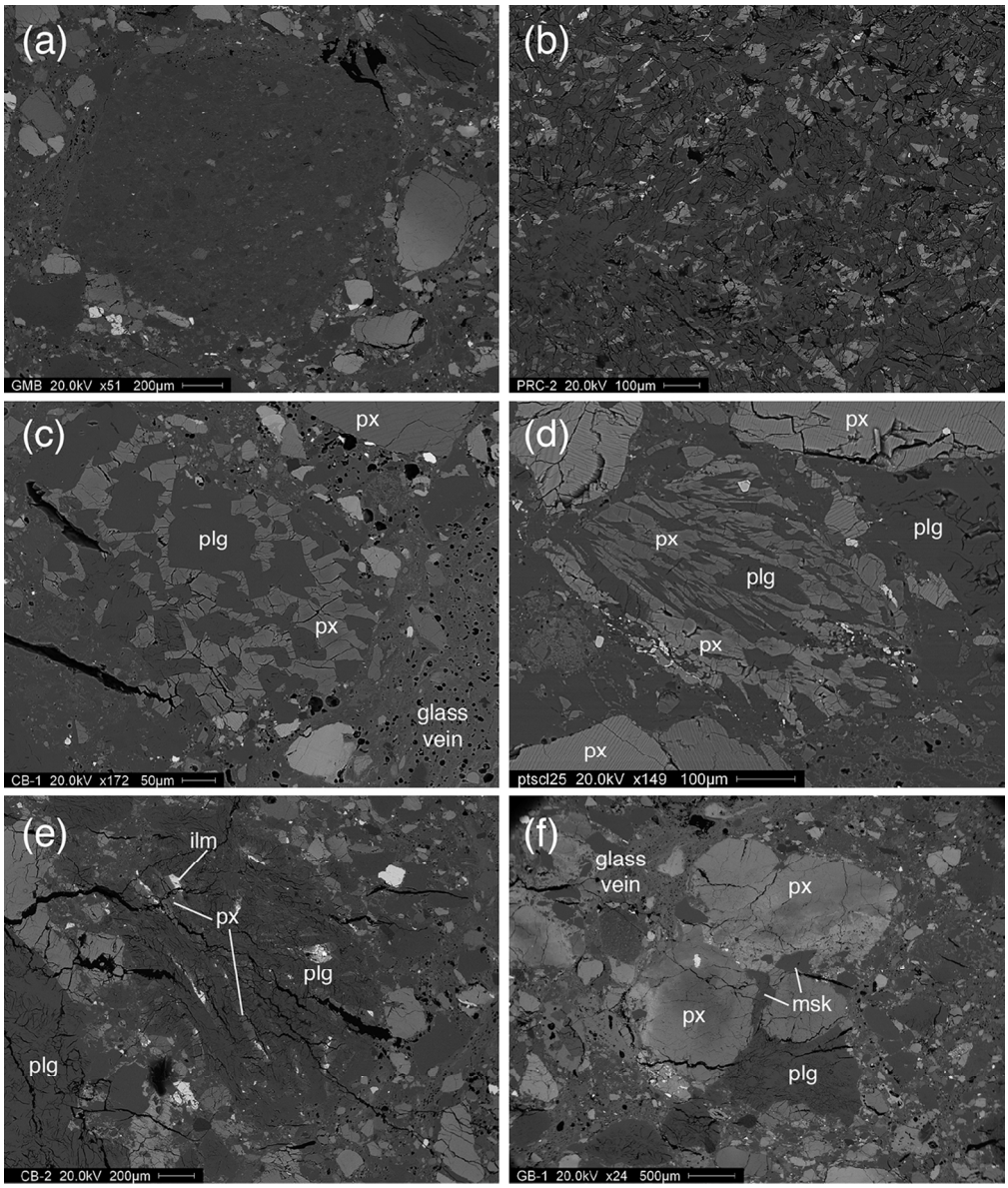

Fig. 4. SEM-BSE images of the most prominent constituents of DEW 12007. a) Glassy melt breccia. b) Plagioclase-rich clast (clast S). c) Microporphyritic pigeonite basalt. d) Sub-variolitic pigeonite basalt. e) Subophitic-glomerophyritic clast (clast 8). f) Gabbroic clast. g) VLT volcanic glass bead. h) Impact glass particle (clast vt 2). i) Symplectitic clinopyroxene-olivine-silica association. j) Fragmental breccia clast (note the chondrule-like object on the left margin of the clast). k) Glass vein with a highly vesiculated region ('quasi-collapsed agglutinate'). l) Vesiculated fusion crust. Abbreviations: ilm = ilmenite; msk = maskelynite; plg = plagioclase; px = pyroxene.
113x133mm (300 x 300 DPI)

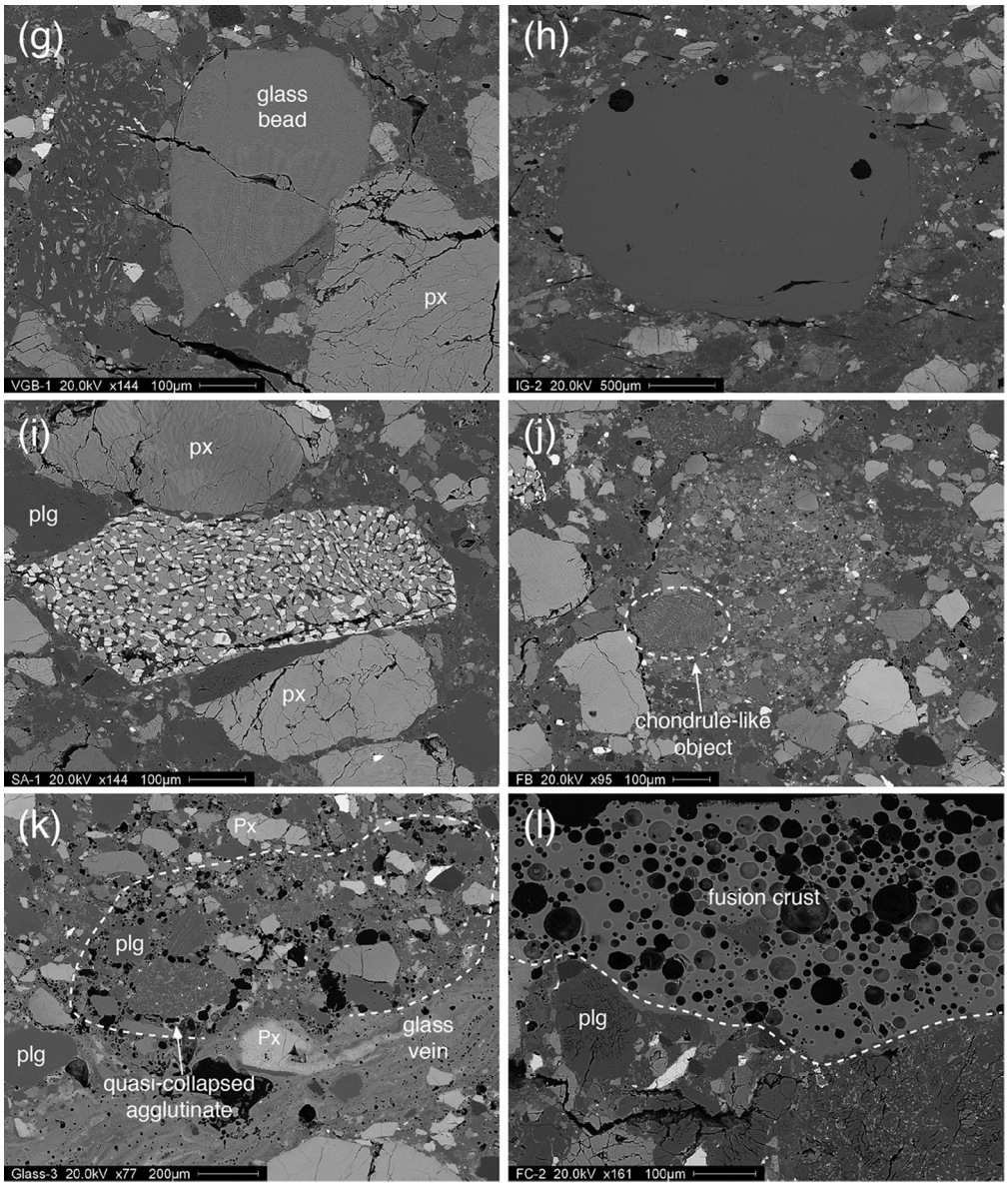

Fig. 4. SEM-BSE images of the most prominent constituents of DEW 12007. a) Glassy melt breccia. b) Plagioclase-rich clast (clast S). c) Microporphyritic pigeonite basalt. d) Sub-variolitic pigeonite basalt. e) Subophitic-glomerophyritic clast (clast 8). f) Gabbroic clast. g) VLT volcanic glass bead. h) Impact glass particle (clast vt 2). i) Symplectitic clinopyroxene-olivine-silica association. j) Fragmental breccia clast (note the chondrule-like object on the left margin of the clast). k) Glass vein with a highly vesiculated region ('quasi-collapsed agglutinate'). l) Vesiculated fusion crust. Abbreviations: ilm = ilmenite; msk = maskelynite; plg = plagioclase; px = pyroxene.
113x132mm (300 x 300 DPI)

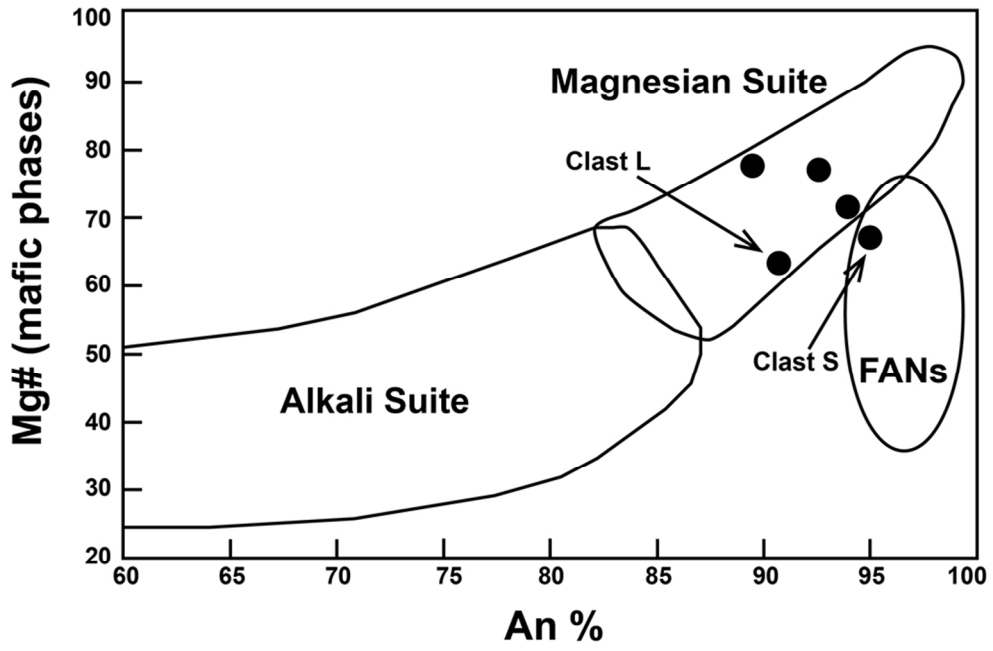

Fig. 5. Mg# (in mafic phases) versus An% (in plagioclase) diagram for the feldspar-rich meta-melt rock clasts in DEW 12007 (see for example Fig. 4b). Compositional fields after Wieckzorek et al. (2006). 88x58mm (300 x 300 DPI)

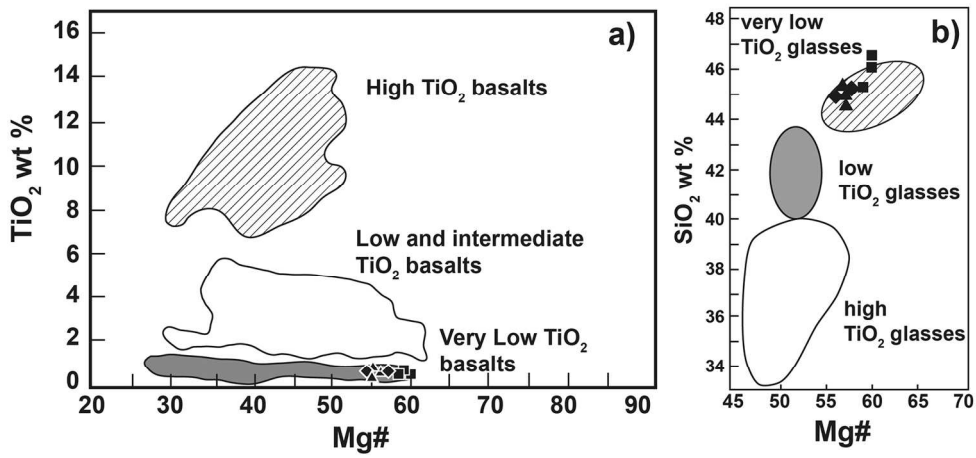

Fig. 6. a) TiO_2 versus Mg# diagram and b) SiO_2 vs Mg# diagram for the volcanic glass beads of DEW 12007. Compositional fields after Papike et al. (1998). Squares, triangles and diamonds represent three different glass bead individuals (see for example Fig. 4g).
155x70mm (300 x 300 DPI)

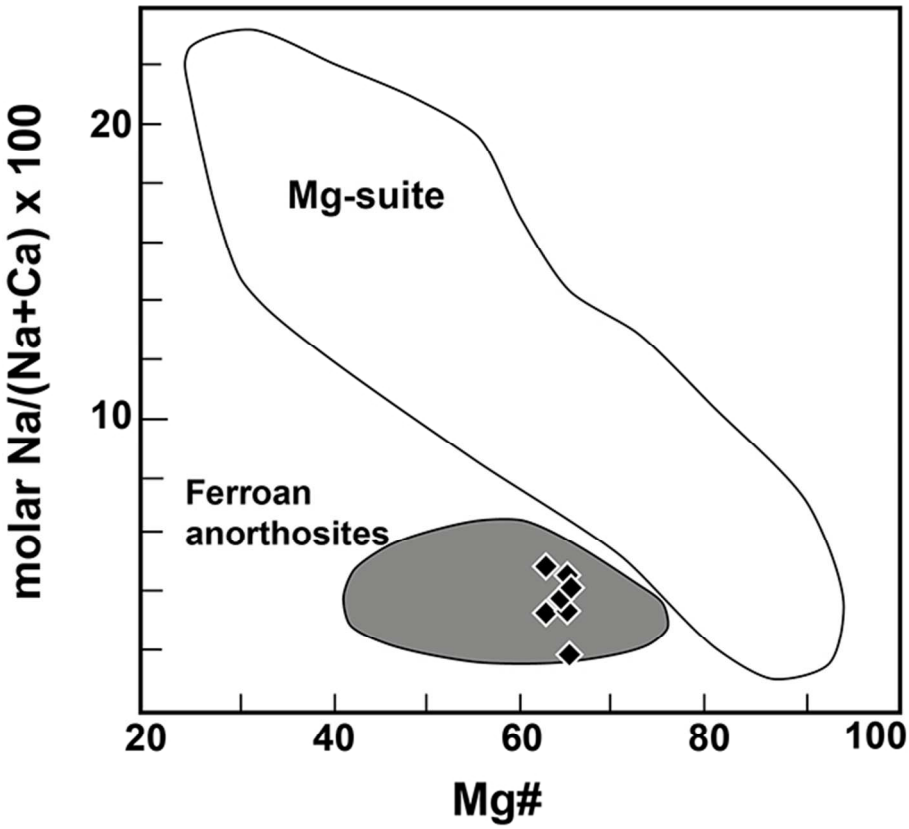

Fig. 7. Molar Na/(Na+Ca) × 100 vs Mg# diagram for the impact glass particle vt 1. Compositional fields for ferroan anorthosites and the Mg-suite rocks after Papike et al. (1998).
66x57mm (300 x 300 DPI)

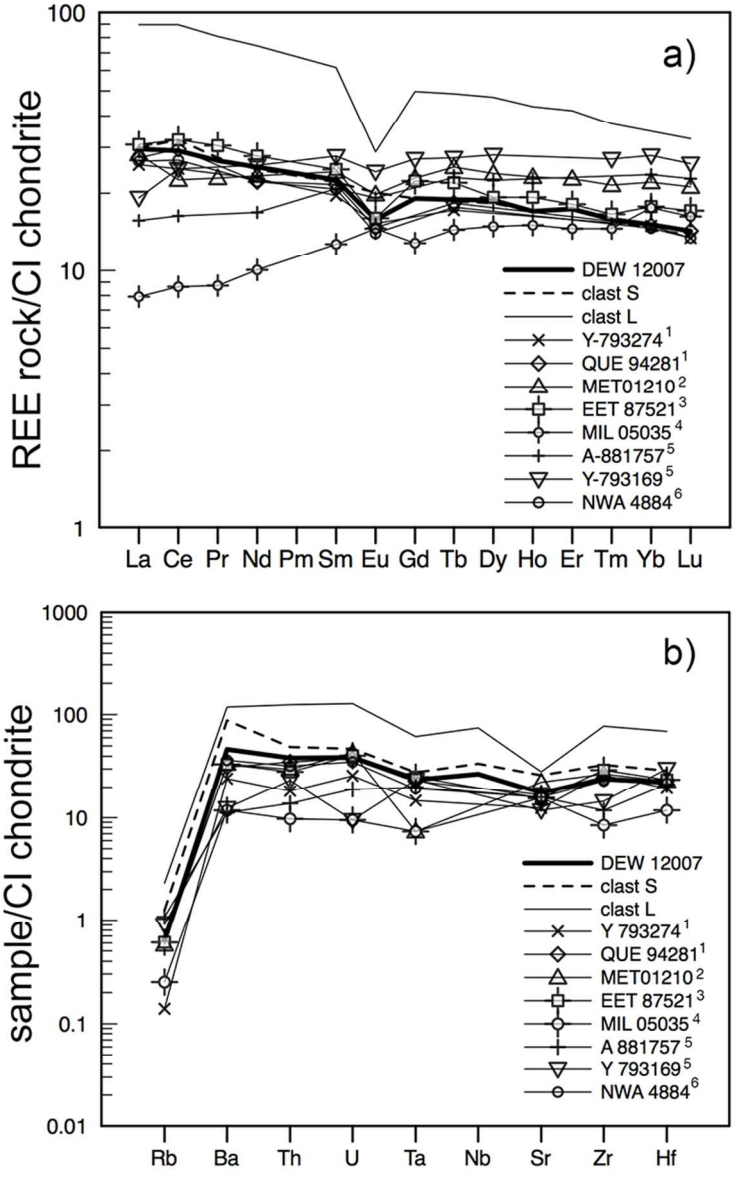

Fig. 8. a) CI chondrite-normalized REE patterns of DEW 12007 (bulk meteorite), clast S, clast L and other lunar meteorites. b) Incompatible element patterns of DEW 12007 (bulk meteorite), clast S, clast L and other lunar meteorites. Normalizing values after McDonough and Sun (1995). Compositional data after: [1]Demidova et al. (2007), [2]Joy et al. (2006), [3]Anand et al. (2003), [4]Liu et al. (2009), [5]Yanai and Kojima (1991), [6]Korotev et al. (2009).
67x106mm (300 x 300 DPI)

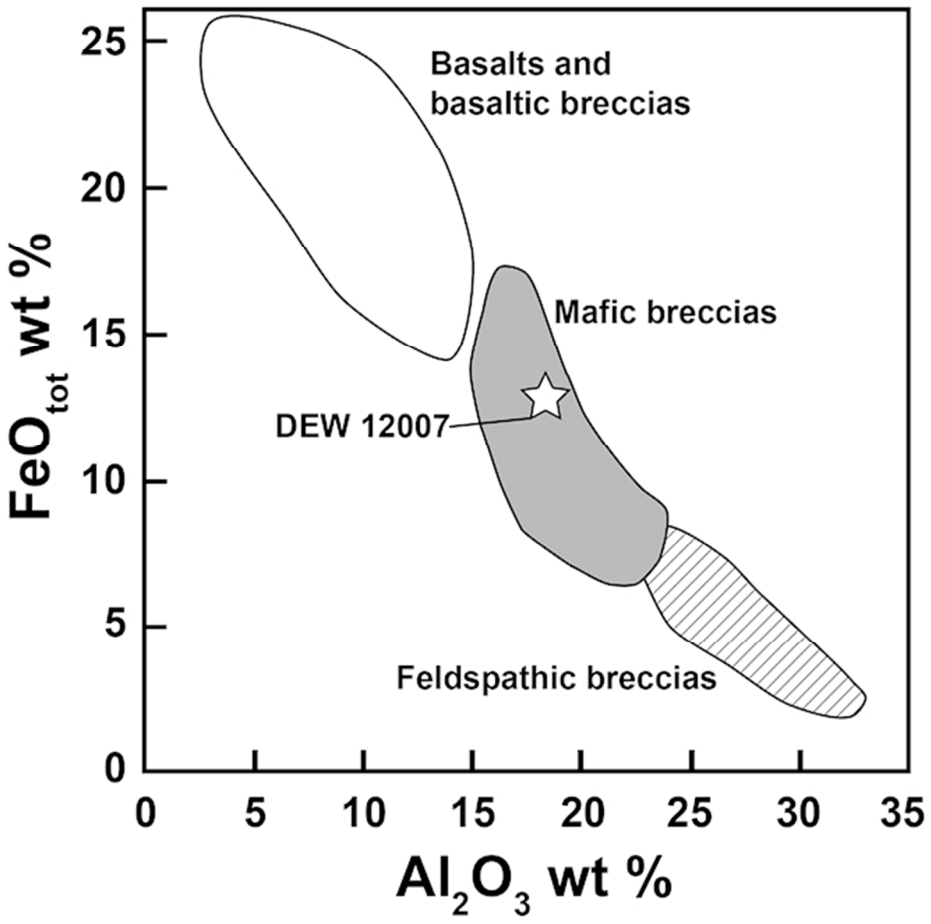

Fig. 9. DEW 12007 in the FeO_{tot} vs Al_2O_3 diagram. Modified after Korotev (http://meteorites.wustl.edu/).
60x59mm (300 x 300 DPI)

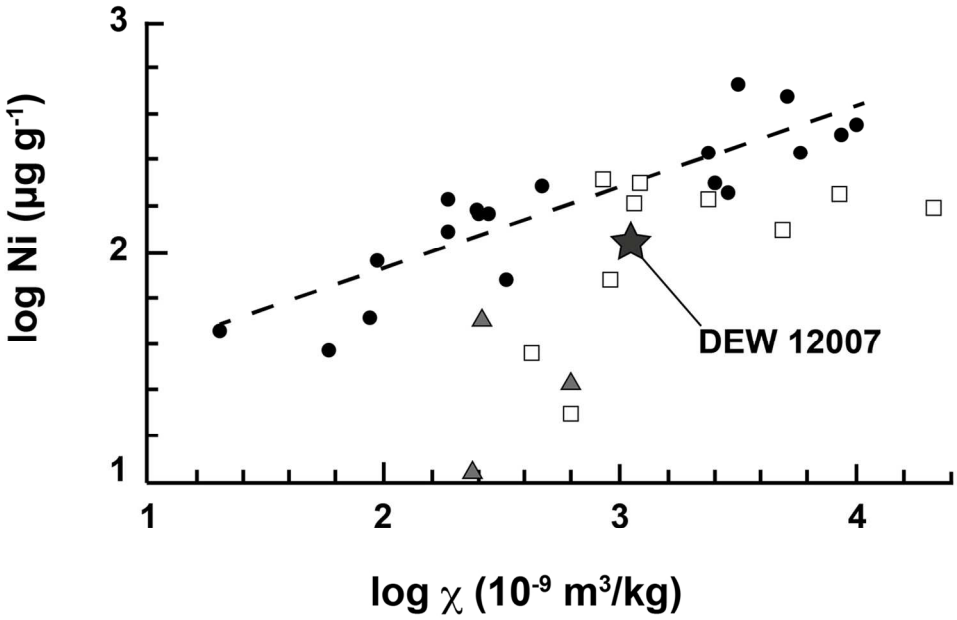

Fig. 10. DEW 12007 in the Log Ni vs Log χ diagram in comparison with other lunar meteorites. Circles: feldspathic breccias; squares: mafic breccias; triangles: basalts. Modified after Rochette et al. (2010).
130x84mm (300 x 300 DPI)

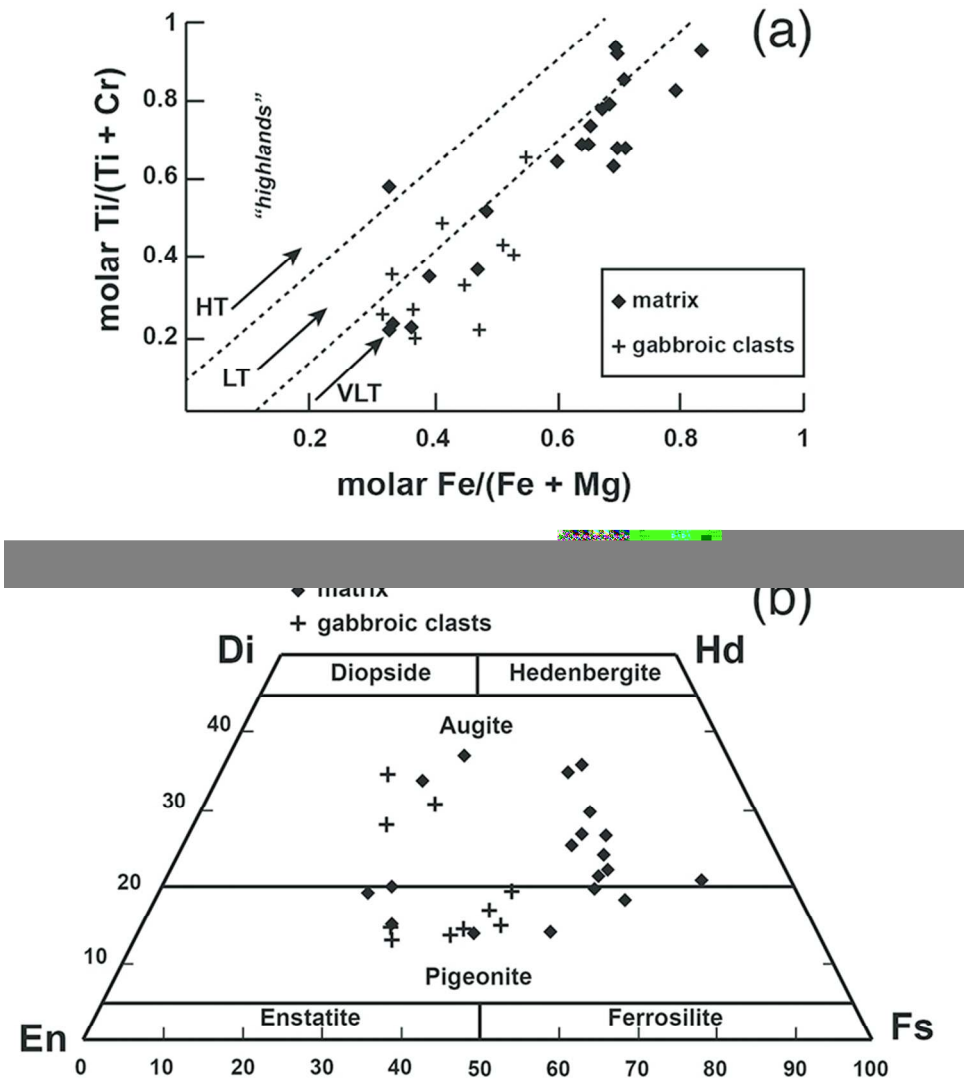

Fig. 11. Mineral chemistry of the pyroxene from gabbroic clasts and the meteorite matrix. a) Ti/(Ti + Cr) vs Fe/(Fe + Mn) diagram. b) Quadrilateral (En-Fs-Di-Hd) pyroxene diagram.
73x91mm (300 x 300 DPI)

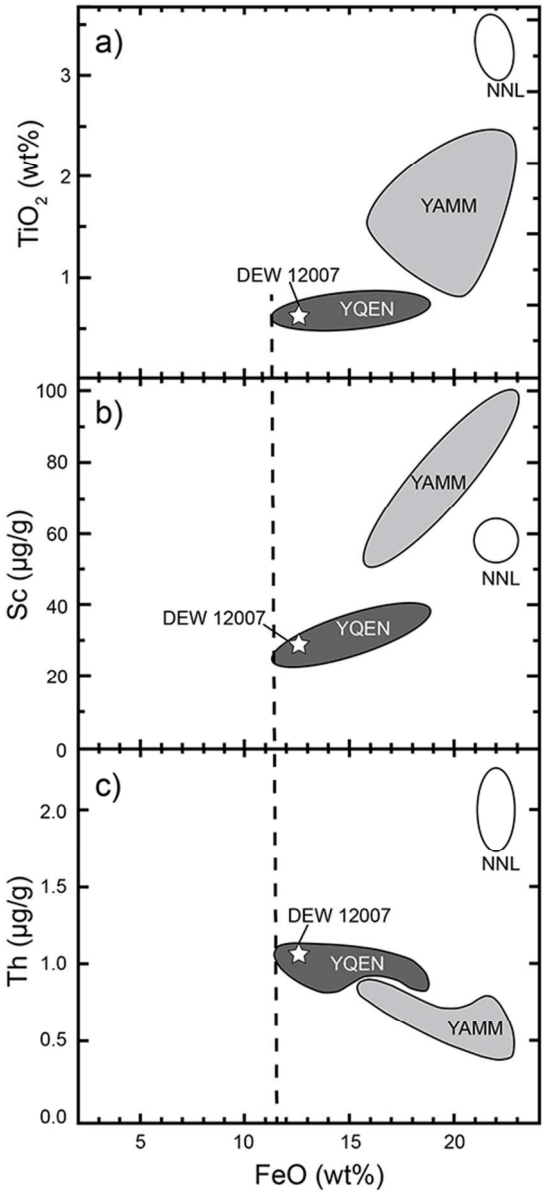

Fig. 12. Scandium, Th, Ti, versus Fe contents in DEW 12007 and other lunar meteorites belonging to the YAMM, NNL, and YQEN putative launch-pairing groups for comparison. The vertical dashed line discriminates between feldspathic and non-feldspathic meteorites. a) Ti vs FeO_{tot} diagram. b) Sc vs FeO_{tot} diagram. c) Th vs FeO_{tot} diagram. Plots modified after Korotev and Zeigler (2014).
48x95mm (300 x 300 DPI)

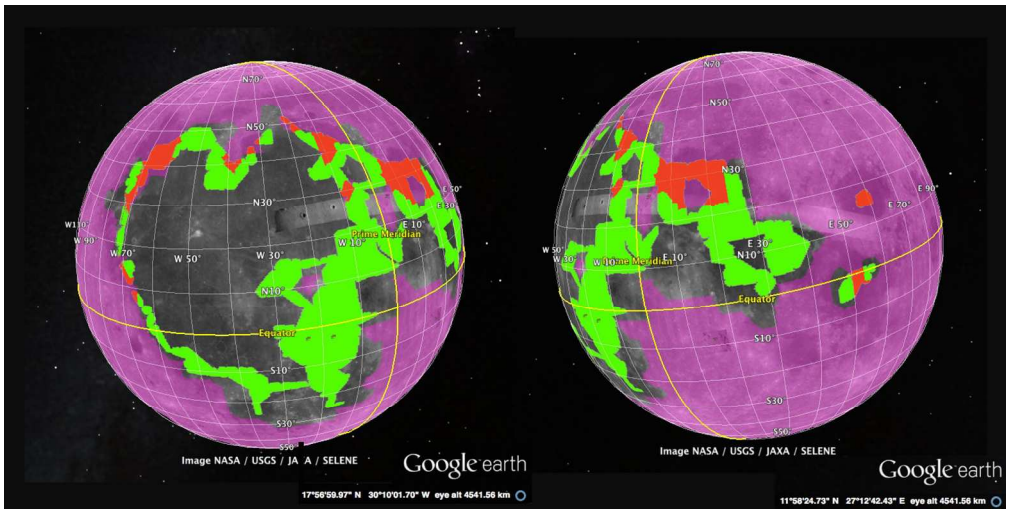

Fig. 13. Search results for FeO between 11.6 and 13.6 wt% (green layer) and TiO_2 below 1.62 wt% (pink layer) using the Clementine datasets. Areas of overlap are red. On the left, the western hemisphere of the Moon; on the right, the eastern hemisphere of the Moon. Images obtained by Google Earth. Mare Serenitatis is located ca. 25°N-35°N, 5°E-25°E.
127x64mm (300 x 300 DPI)

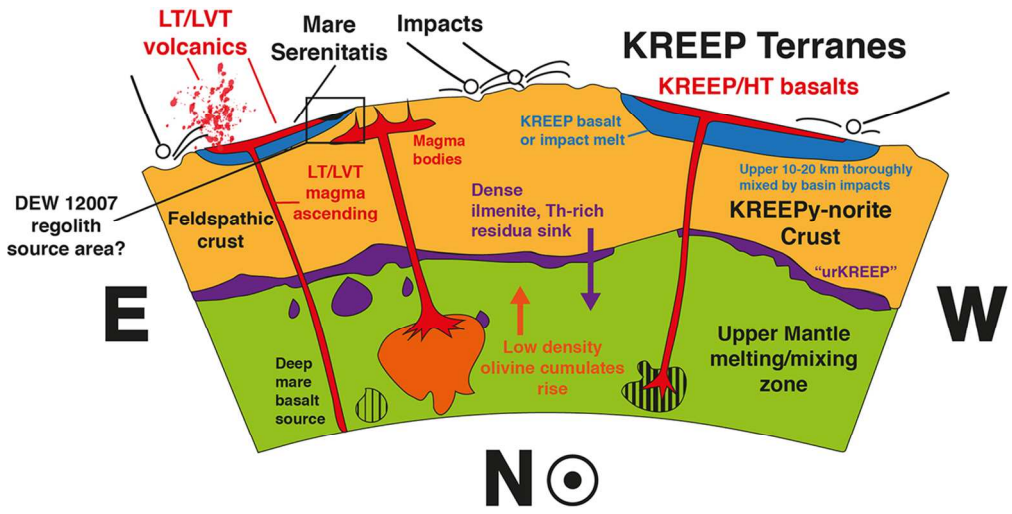

Fig. 14. In this image, modified after Taylor (2000), the regolith sampled by DEW 12007 is contextualized in a schematic section of the lunar northern hemisphere crust and upper mantle passing through the northern basins (Oceanus Procellarum, Mare Imbrium, and Mare Serenitatis).
110x59mm (300 x 300 DPI)

Table 1. Bulk physical properties and oxygen isotope data for DEW 12007.

Bulk density ρ_b (g cm^{-3})	2.90 ± 0.01
Grain density ρ_g (g cm^{-3})	3.02 ± 0.03
Porosity η_t (vol.%)	4.1 ± 1.1
Log χ (10^{-9} m^3 kg^{-1})	3.11 ± 0.9
$\delta^{18}O$	6.05 ‰
$\delta^{17}O$	3.13 ‰
$\Delta^{17}O$	-0.075 ‰

Table 2. Inventory of the DEW 12007 constituents and their mineralogy.

Class of constituents	Grain size (G) and abundance (A)	Texture	First-order mineralogy and composition	Hypothesized genesis
Glassy impact-melt breccias	G: 1-5mm A: ~15%	Crystalline and lithic fragments embedded in a vitrophyric matrix	Relict phases: plg, cpx, ol; matrix: glass (plg where cryptocrystalline)	Medium-sized episodes of local melting
Plagioclase-rich clasts	G: 1-5 mm A: ~10%	microphenoxls (>50%) embedded in a mafic matrix	Plg microphenoxls; matrix: cpx, glass ± ox (ilm, bdy), Fe,Ni-metal, sulfides, phosphides	Mare-related volcanic rocks with LT and VLT affinities
Crystalline basalts	G: <1 mm A: ~5%	hypocrystalline to holocrystalline, hyalopilitic to microglomerophyritic, microporphyritic to intergranular, ophitic and variolitic	Plg, cpx ± ox, glass	Mare-related volcanic rocks with LT and VLT affinities
Gabbros	G: ~2-3 mm A: ~5%	Holocrystalline, microphaneritic, granular, consertal	Cpx, plg, si; minor chr, trq, bdy, phosphides, melt inclusions (?)	Shallow intrusion within a mare-related VLT volcanic complex
Volcanic glasses	G: ~0.5 mm A: ~1%	Homogeneous glass beads, rare heuedral xls	Picritc glass, microxls of forsteritic ol	Mare-related pyroclastic products with VLT affinities
Impact glasses	G: ~2-3 mm A: ~1%	Ellipsoidal homogeneous glass particles	High-alumina glass	Impact glass splashes, nonmare-related source rocks
Cpx-ol-si symplectites	G: ≤0.5 mm A: ~1%	Symplectitic, with sandwich-like microstructures	Cpx, ol, si ± ilm, high-K, high-Si glass	Exsolution of metastable cpx with intermediate Ca contents
Fragmental breccias	G: ~0.6 mm A: <1%	Microbrecciated clasts	Mainly plg, cpx, ol (forsteritic)	Lithification of fragmental ejecta
Mineral fragments of the matrix	G: ≤0.5 mm A: ~40%	Monocrystalline angular fragments with seriate distribution	Cpx, plg, ol, si, ox (ilm, chr, usp, bdy), Fe,Ni-metal, sulfides, phosphides, phosphates	Most silicates can be associated to the gabbros and basalts; the HSE-bearing phases have mainly a meteoritic origin
Glass veins	G: ~0.1 vs ~1 mm A: pervasive	Vesiculated and heterogeneous, with flow microstructures	Al-rich mafic glass; bulk composition similar to that of the bulk rock	Impact glass generated *in situ*; it cements the meteorite
Agglutinates	G: ~0.5 mm A: ~1%	Aggregates of mineral fragments cemented by highly vesiculated glass	Mineralogy and glass composition indistinguishable from the rest of the matrix	Circumstantiate episodes of melting due to micrometeorite impact
Fusion crust	G: ~0.3 mm thick A: isolated relicts	External amorphous, highly vesiculated and scoriaceous covering, with relict minerals and skeletal neoformation xls	Glass: composition similar to that of the glassy veins; relicts: plg, cpx, ox; neoformation phases: ol (fo), ox (mag?), Fe,Ni metal	Superficial melting of the meteorite during the ablative passage through the atmosphere

Abbreviations: plg=plagioclase; cpx=clinopyroxene; ol=olivine; ox=oxide; ilm=ilmenite; bdy=baddeleyite; chr=chromite; trq=tranquillityite; usp=ulvöspinel; mag=magnetite; si=silica phase; xls=crystals.

Table 3. Chemical composition (oxide wt%) of Al-rich glasses from feldspathic clasts of DEW 12007 and from the lunar meteorite Y 86032. Analyses by EPMA.

	DEW 12007 (this work)			Y 86032 (Koeberl et al. 1990)		
	Clast S	Clast L	Clast L			
SiO_2	38.3	46.2	40.1	44.4	42.8	43.3
TiO_2	0.09	0.47	0.37	0.17	0.05	0.11
Al_2O_3	13.3	26.1	25.8	20.8	20.4	17.8
Cr_2O_3	b.d.l.	0.14	0.17	0.05	0.11	0.05
MgO	19.7	4.52	6.37	11.1	10.7	16.3
CaO	5.70	16.9	14.7	12.5	12.0	10.0
MnO	0.29	0.10	0.05	0.12	0.17	0.16
FeO_{tot}	22.4	5.16	11.5	9.6	12.1	13.8
NiO	0.04	0.01	0.27	n.d.	n.d.	n.d.
Na_2O	0.32	0.59	0.42	0.68	0.52	0.54
K_2O	0.06	0.09	0.05	b.d.l.	b.d.l.	b.d.l.
Total	100.2	100.3	99.8	99.4	98.9	102.1
Mg#	61.0	61.0	49.7	67.3	61.1	60.1

Abbreviations: b.d.l. = below detection limit; n.d. = not determined.

Table 4. Chemical composition (oxide wt%) of plagioclase from basaltic clasts, gabbroic clasts and the matrix of DEW 12007. Analyses by EPMA.

	Basaltic clasts					Gabbroic clasts					Matrix				
	LT	VLT	Cl 8												
SiO_2	43.8	45.7	45.1	43.9	45.7	45.6	45.5	45.5	44.6	45.2	44.4	44.3	43.6	45.5	45.3
Al_2O_3	35.7	30.4	34.6	33.9	33.7	33.7	34.1	33.9	34.0	33.6	35.2	35.0	35.4	34.9	33.7
MgO	0.06	1.52	0.30	0.32	0.50	0.23	0.21	0.19	0.21	0.24	0.03	0.05	0.06	0.04	0.44
CaO	19.4	17.3	18.7	18.3	17.7	18.7	18.5	18.5	18.9	18.6	18.6	19.2	19.5	18.1	17.8
FeO_{tot}	0.20	3.70	0.20	0.57	0.96	0.52	0.65	0.55	0.56	0.56	0.29	0.27	0.19	0.40	0.89
Na_2O	0.67	0.88	0.87	0.71	0.92	0.67	0.80	1.00	0.75	0.79	0.88	0.70	0.36	1.15	1.14
K_2O	0.04	0.09	0.08	0.06	0.19	0.01	0.02	0.03	b.d.l.	0.03	0.05	0.06	b.d.l.	0.10	0.02
Total	99.9	99.6	99.9	97.8	99.7	99.4	99.8	99.7	99.0	99.0	99.5	99.6	99.1	100.2	99.3
An%	94.0	91.1	91.8	93.1	90.4	93.9	92.7	90.9	93.3	92.7	91.8	93.5	96.8	89.2	95.4

Abbreviations: b.d.l. = below detection limit; n.d. = not determined.

Table 5. Chemical composition (oxide wt%) of pyroxene from gabbroic clasts, basaltic clasts, and the matrix of DEW 12007. Analyses by EPMA.

	Gabbroic clasts				Basaltic clasts			Matrix						
					LT	VLT	Cl 8							
SiO_2	52.1	51.3	50.0	50.6	51.6	51.2	52.5	51.9	51.4	50.8	50.9	48.1	48.2	48.0
TiO_2	0.19	0.25	0.30	0.29	0.59	0.39	0.55	0.19	0.33	1.08	0.26	0.66	1.00	0.66
Al_2O_3	1.31	1.67	0.89	1.02	1.13	1.07	1.19	1.35	1.42	1.54	1.10	1.18	0.92	0.92
Cr_2O_3	0.50	0.70	0.42	0.49	0.63	0.17	0.28	0.63	0.57	0.75	0.43	0.23	0.26	0.30
MgO	18.9	13.6	13.7	15.4	19.6	18.1	23.6	19.1	14.7	15.3	15.4	9.2	7.6	7.4
CaO	7.24	16.8	7.09	6.93	5.93	5.96	4.35	6.91	14.2	16.3	7.24	8.35	12.2	9.70
MnO	0.33	0.31	0.45	0.36	0.33	0.20	0.30	0.33	0.30	0.24	0.42	0.43	0.40	0.38
FeO_{tot}	19.3	12.8	27.0	24.4	19.6	21.6	16.1	19.5	16.8	13.3	24.5	31.1	28.5	32.1
NiO	b.d.l.	b.d.l.	b.d.l.	b.d.l.	b.d.l.	0.03	b.d.l.	0.04	b.d.l.	b.d.l.	b.d.l.	0.04	0.02	0.03
Na_2O	0.04	0.02	0.02	0.02	0.04	0.01	0.01	0.03	0.04	0.09	0.04	0.02	0.06	0.05
Total	99.9	97.5	99.9	99.5	99.5	98.7	98.9	100.0	99.8	99.4	100.3	99.3	99.2	99.5
Mg#	63.6	68.4	47.4	52.8	64.1	59.9	72.4	63.5	60.9	67.2	52.8	34.5	32.1	29.0

Abbreviations: b.d.l. = below detection limit; n.d. = not determined.

Table 6. Chemical composition (oxide wt%) of volcanic glass beads of DEW 12007 in comparison with the Apollo 17 VLT glasses analyzed by Shearer and Papike (1993). Analyses by EPMA.

	DEW 12007 (this work)			Apollo Samples	
				A 17, VLT	A 17, VLT
SiO_2	45.1	45.1	46.0	46.3	46.0
TiO_2	0.50	0.53	0.49	0.55	0.86
Al_2O_3	10.0	9.5	10.4	9.8	10.2
Cr_2O_3	0.54	0.56	0.45	0.46	0.54
MgO	14.4	14.8	15.1	14.1	13.8
CaO	9.24	9.03	9.20	9.41	9.86
MnO	0.26	0.25	0.24	0.30	0.24
FeO_{tot}	19.4	19.7	18.2	19.5	18.8
Na_2O	0.14	0.22	0.26	0.16	0.23
K_2O	0.01	0.04	0.02	0.01	b.d.l.
Total	99.6	99.7	100.4	100.6	100.5
Mg#	56.9	57.2	59.6	56.3	55.4

Abbreviations: b.d.l. = below detection limit; n.d. = not determined.

Table 7. Chemical composition (oxide wt%) of two impact glasses from DEW 12007 in comparison with some Apollo impact glasses and ferroan anorthosites. Analyses by EPMA.

	Impact glass particles				FAN Anorthosites (Apollo Samples)		
	DEW 12007 (this work)		Apollo Samples				
	Vt 1	Vt 2	*I*	*II*	*III*	*IV*	*V*
SiO_2	43.7	49.5	44.9	44.2	45.3	43.3	45.3
TiO_2	0.42	1.90	0.28	0.64	0.12	n.d.	0.40
Al_2O_3	29.4	20.4	29.2	27.8	28.0	29.7	26.2
Cr_2O_3	0.06	0.18	0.08	0.10	0.09	0.07	0.08
MgO	4.77	10.1	4.72	5.09	3.85	3.80	5.30
CaO	16.8	12.0	16.5	15.7	16.8	17.4	15.8
MnO	0.06	0.08	n.d.	n.d.	0.07	0.06	0.09
FeO_{tot}	4.42	5.03	3.79	5.02	4.77	4.00	6.56
Na_2O	0.38	0.04	0.44	0.47	0.29	0.21	0.28
K_2O	0.06	0.04	0.09	0.14	0.02	0.02	0.02
Total	100.1	99.3	100.0	99.2	99.3	98.6	100.0
Mg#	66.0	78.3	68.9	64.8	59.0	62.9	59.0

Apollo data after: [I]60639.34, Morris et al. (1986); [II]67115.17, Taylor et al. (1973); [III]15363.1, Warren et al. (1987); [IV]62236.9, Warren and Wasson (1978); [V]67016.326/8, Norman and Taylor (1992). Abbreviations: b.d.l. = below detection limit; n.d. = not determined.

Table 8. Chemical composition (oxide wt%) of some non-silicate mineral fragments from the matrix of DEW 12007. Analyses by EPMA.

	Oxides					Metal alloys & sulfides		
	Ilmenite	Chromite	Ülvospinel	Baddeleyite		Fe-Ni metal		Troilite
SiO_2	0.07	0.17	0.04	0.22	Si	0.02	0.73	0.02
TiO_2	52.8	4.23	29.0	0.70	P	b.l.d	b.d.l.	b.d.l.
ZrO_2	0.20	0.10	b.d.l.	92.7	S	0.04	0.03	36.4
Al_2O_3	b.d.l.	14.9	4.15	b.d.l.	Ti	0.02	0.01	b.d.l.
Cr_2O_3	0.10	44.0	5.65	b.d.l.	Cr	b.d.l.	0.04	b.d.l.
MgO	0.63	3.97	0.47	0.06	Mn	b.d.l.	0.01	0.03
CaO	0.14	0.03	0.02	1.54	Fe	93.3	56.6	62.7
MnO	0.39	0.35	0.32	b.d.l.	Co	0.57	4.66	b.d.l.
FeO_{tot}	45.4	31.6	59.8	3.01	Ni	5.00	33.9	0.04
NiO	b.d.l.	b.d.l.	b.d.l.	b.d.l.	Cu	0.04	0.60	0.03
					Zn	0.07	0.01	b.d.l.
Total	99.7	99.4	99.5	98.2	Total	99.1	96.6	99.2

Abbreviations: b.d.l. = below detection limit; n.d. = not determined.

Table 9. Chemical composition (oxide wt%) of two glassy veins from DEW 12007. Analyses by EPMA.

	Vein 1	Vein 2
SiO_2	46.5	45.6
TiO_2	1.09	0.55
Al_2O_3	16.9	25.0
Cr_2O_3	0.19	0.09
MgO	5.96	5.89
CaO	13.4	15.2
MnO	0.21	0.10
FeO_{tot}	14.9	7.14
Na_2O	0.44	0.50
K_2O	0.07	0.08
Total	99.8	100.1
Mg#	42.7	59.4

Table 10. Comparison between the chemical composition of the fusion crust (FC) of DEW 12007 and its bulk composition (bulk).

$(Al/Si)_{FC}/(Al/Si)_{bulk}$	1.04
$(Ti/Si)_{FC}/(Ti/Si)_{bulk}$	0.99
$(Ca/Si)_{FC}/(Ca/Si)_{bulk}$	1.00
$(Mg/Si)_{FC}/(Mg/Si)_{bulk}$	1.00
$(Fe/Si)_{FC}/(Fe/Si)_{bulk}$	0.84
$(Fe/Mn)_{FC}/(Fe/Mn)_{bulk}$	0.89

Table 11. Major-element bulk composition (wt%) of DEW 12007. Analyses by Fusion-XRF.

SiO_2	46.3
TiO_2	0.62
Al_2O_3	18.3
FeO_{tot}	12.6
MnO	0.163
MgO	8.13
CaO	12.9
Na_2O	0.40
K_2O	0.08
P_2O_5	0.07
LOI	-0.86

Table 12. Trace-element bulk composition (μg g^{-1}) of DEW 12007 (average of two replicate analyses), clast S and clast L. Analyses by ICP-MS.

	DEW 12007		
	Bulk	Clast S	Clast L
Li	7.2	4.9	13.4
Be	0.70	0.83	1.95
Sc	28.8	10.5	1.95
V	88	20	28
Cr	1654	559	710
Co	36	19.6	14.6
Ni	135	156	127
Cu	9.1	46	8.8
Ga	4.5	3.5	4.3
Rb	1.45	2.93	5.3
Sr	127	189	204
Y	26.5	25.6	66
Zr	91.6	125	298
Nb	6.4	8.1	17.8
Ba	112	213	284
La	7.0	7.1	21.2
Ce	18.1	19.7	55
Pr	2.51	2.54	7.5
Nd	11.6	11.3	34
Sm	3.31	3.26	9.1
Eu	0.90	1.13	1.62
Gd	3.8	3.8	9.9
Tb	0.68	0.67	1.76
Dy	4.61	4.50	11.58
Ho	0.96	0.93	2.37
Er	2.80	2.79	6.7
Tm	0.40	0.39	0.92
Yb	2.44	2.32	5.6
Lu	0.35	0.34	0.80
Hf	2.28	2.96	7.1
Ta	0.32	0.38	0.84
W	0.18	0.30	0.35
Pb	1.61	1.91	3.4
Th	1.11	1.41	3.6
U	0.29	0.35	0.95